

Magnetic, thermal, and electronic properties of iron-antimony filled skutterudites $M\text{Fe}_4\text{Sb}_{12}$ ($M=\text{Na}, \text{K}, \text{Ca}, \text{Sr}, \text{Ba}, \text{La}, \text{Yb}$)

W. Schnelle,¹ A. Leithe-Jasper,^{1,*} H. Rosner,¹ R. Cardoso-Gil,¹ R. Gumeniuk,¹ D. Trots,² J. A. Mydosh,^{1,†} and Yu. Grin¹

¹Max-Planck-Institut für Chemische Physik fester Stoffe, Nöthnitzer Straße 40, 01187 Dresden, Germany

²HASYLAB at DESY, Notkestraße 85, 22603 Hamburg, Germany

(Received 14 November 2007; revised manuscript received 30 January 2008; published 19 March 2008)

The magnetic susceptibility, field-dependent heat capacity, and electrical transport properties (resistivity and Hall effect) are investigated for filled skutterudites $M\text{Fe}_4\text{Sb}_{12}$ with $M=\text{Na}, \text{K}, \text{Ca}, \text{Sr}, \text{Ba}, \text{Yb}$, and La . The specific heat $c_p(T)$ reveals linear terms γ ranging from 100 to 200 mJ mol⁻¹ K⁻². An Einstein term contributing to $c_p(T)$ is analyzed and discussed in connection with thermal vibrations of the cations M . The Einstein temperatures $\Theta_E=70\text{--}105$ K are compared with values derived from atomic displacement parameters obtained by x-ray diffraction and other methods. Deviations of the amplitude and frequency of the Einstein term from the expected values are discussed. The paramagnetic susceptibility and the magnetic ground state varies systematically with the cation charge. While $\text{NaFe}_4\text{Sb}_{12}$ and $\text{KFe}_4\text{Sb}_{12}$ are nearly half-metallic weak itinerant ferromagnets with $T_C\approx 80$ K, $\text{CaFe}_4\text{Sb}_{12}$, $\text{SrFe}_4\text{Sb}_{12}$, $\text{BaFe}_4\text{Sb}_{12}$, and $\text{YbFe}_4\text{Sb}_{12}$ are nearly ferromagnetic metals with a high Sommerfeld-Wilson ratio and strong ferromagnetic spin fluctuations. $\text{LaFe}_4\text{Sb}_{12}$ is paramagnetic with predominantly antiferromagnetic fluctuations. The decrease of the low-temperature specific heat with magnetic field is investigated. A large positive magnetoresistance is observed for both ferromagnetic and nearly ferromagnetic compounds, while that of the La compound is small. Size and temperature dependence of the Hall coefficient points to a compensation of hole and electron carriers. The temperature dependence of the resistivity displays different characteristic power laws and an anomaly around 80 K. These observations can be explained by details of the electronic structure. A systematic variation of the properties with charge transfer from the cation M to the $[\text{Fe}_4\text{Sb}_{12}]$ polyanion is recognized.

DOI: 10.1103/PhysRevB.77.094421

PACS number(s): 75.50.Bb, 75.40.Cx, 71.20.Lp

I. INTRODUCTION

The filled skutterudites exhibit a wealth of topical behaviors, which are the source and motivation of increasing interest and efforts to study and understand the underlying physics. All these materials derive from the mineral skutterudite $(\text{Co}, \text{Fe}, \text{Ni})\text{As}_{2-3}$. Binary skutterudites having the general chemical formula TX_3 are formed by the members of the ninth group of the periodic system ($T=\text{Co}, \text{Rh}, \text{Ir}$) with pnictogens ($X=\text{P}, \text{As}, \text{Sb}$). No binary compounds with iron, ruthenium, and osmium could be synthesized under equilibrium conditions. In order to stabilize such compounds it is necessary to include electropositive elements as a third component leading to the total formula $M_y\text{T}_4\text{X}_{12}$.¹ Here, M can be an alkali, alkaline-earth, rare-earth, actinide metal, or thallium. Different degrees of filling y can be realized up to $y=1$; however, the real limits for y depend strongly on the “filler” M and the “host” $[\text{T}_4\text{X}_{12}]$ and are not yet well explored. The compounds $M_y\text{T}_4\text{X}_{12}$ are also called “filled skutterudites” since the stabilizing atoms reside in large voids already present in the transition-metal pnictogen framework.¹

A variety of properties has been observed for rare-earth filled skutterudites ranging from metal-insulator transitions to magnetic and quadrupole orderings, conventional and unconventional superconductivities, heavy fermion and/or non-Fermi liquid behavior, and fluctuating and/or mixed valency.²⁻⁵ Furthermore, interest in these compounds is fueled by their possible use in thermoelectric applications.^{6,7} For exhaustive reviews on the skutterudites physics and chemistry we refer to Refs. 2 and 7. All these studies suggest that the physics of filled skutterudites is governed by a subtle interplay of the filler ions and their transition-metal-pnictogen host structure.

In this paper, we present a comprehensive study of the structural, thermal, electronic, and transport properties of filled skutterudites, where the fillers are nonmagnetic metals. The recently synthesized skutterudites $\text{NaFe}_4\text{Sb}_{12}$ and $\text{KFe}_4\text{Sb}_{12}$, and newly discovered isostructural $\text{TlFe}_4\text{Sb}_{12}$ exhibit ferromagnetic order below $T_C\approx 80$ K with weak itinerant magnetic moments and strong spin fluctuations (SFs).⁸⁻¹⁰ These compounds are nearly half-metallic ferromagnets, which are promising materials for spin-electronic devices (spintronics).¹¹ A large spin polarization was predicted from band structure calculations^{9,10} and, actually, a large charge carrier spin polarization (up to 67%) was found experimentally by point contact spectroscopy.¹²

The alkaline-earth metal compounds ($M=\text{Ca}, \text{Sr}, \text{Ba}$) previously studied by Danebrock *et al.*¹³ stay paramagnetic down to 2 K. However, our electronic structure calculations indicate that the ground state should be also ferromagnetic within the local density approximation.¹⁴ The ytterbium-filled skutterudite $\text{Yb}_y\text{Fe}_4\text{Sb}_{12}$ is a special case. Recently,¹⁵ it was shown that Yb in this compound is stable divalent and its properties are *not* due to the formation of a heavy-electron state at low temperatures by the Kondo effect. Consequently, the previous classification of $\text{YbFe}_4\text{Sb}_{12}$ as a heavy-fermion system is not justified. Interestingly, the electronic properties of $\text{Yb}_y\text{Fe}_4\text{Sb}_{12}$, $\text{CaFe}_4\text{Sb}_{12}$, and $\text{BaFe}_4\text{Sb}_{12}$ are found to be almost identical. All three compounds have a huge Sommerfeld-Wilson ratio and display large ferromagnetic spin fluctuations, demonstrating that they are close to the ferromagnetic quantum critical point.^{9,16-18} The nearly ferromagnetic compounds exhibit a pseudogap in the infrared optical conductivity which appears at temperatures below ~ 100 K.¹⁹ This common phenomenon could be traced back

to certain sharp structures in the band structure closely above E_F ; thus, the occurrence of such a pseudogap does not require the presence of strong electronic correlations.¹⁹

Data for the compound $\text{La}_y\text{Fe}_4\text{Sb}_{12}$ ($y=0.79$, $y=0.92$) complete our study. Lanthanum is stable trivalent and the occupancy of the skutterudite's icosahedral void with this ion seems to be variable ($y \leq 1$).

With this set of cations possessing charges 1+, 2+, and 3+, an electron input to the $[\text{Fe}_4\text{Sb}_{12}]$ host between 1.00 and max. 2.76 could be realized. This charge transfer leads to systematic modifications of the electronic states. This, together with the widely varying masses and radii of these cations, leads to a systematic change of the phononic spectrum of the crystal. Therefore also the elastic properties, as, e.g., expressed in the Debye temperature, are altered and an influence on the thermal transport properties could be expected.

Section II will describe the synthesis of the compounds and our experimental techniques. In Sec. III A we show results for the site occupancy, the lattice size, and the atomic displacement parameters of the individual cations. A short review of the magnetic properties of the compounds (Sec. III B) is supplemented by new magnetization data on $\text{La}_y\text{Fe}_4\text{Sb}_{12}$ single crystals and a $\text{SrFe}_4\text{Sb}_{12}$ sintered sample. Specific heat capacity, its contributions, and its magnetic field dependence will be analyzed in detail in Secs. III C–III E. Electrical (magneto)resistivity and Hall effect data are discussed in Secs. III F and III G. In Sec. IV the results on $M_y\text{Fe}_4\text{Sb}_{12}$ with the differently charged cations M are summarized.

II. EXPERIMENT

A. Synthesis

The synthesis of the polycrystalline samples of $M\text{Fe}_4\text{Sb}_{12}$ ($M=\text{Na}, \text{K}, \text{Ca}, \text{Ba}$) was already described in Ref. 9, that of the Yb compound single crystals in Ref. 15. Polycrystalline material of the Sr compound was made similarly. Crystals of $\text{La}_y\text{Fe}_4\text{Sb}_{12}$ with 3–5 mm size were synthesized in antimony flux. Crystals of $\text{SrFe}_4\text{Sb}_{12}$ (typical size of 0.5 mm) and $\text{BaFe}_4\text{Sb}_{12}$ (typical size of 1 mm) with large (100) and smaller (110) faces were grown by the same method. In addition, polycrystalline pellets and several single crystals of $\text{Yb}_y\text{Fe}_4\text{Sb}_{12}$ (y near unity) were investigated in order to find a sample with minimum content of Yb_2O_3 . This magnetically ordering Yb^{3+} -containing impurity shows up clearly only in the low-temperature specific heat as a lambda peak (or broadened maximum) at 2.3 K.^{20,21} Photoemission and x-ray absorption spectroscopic measurements prove that the oxide is located predominantly on the surface of the grains.²² $\text{La}_y\text{Fe}_4\text{Sb}_{12}$ crystals with different filling levels y were investigated since these materials showed different behaviors in the electronic heat capacity and its magnetic field dependence. It is not clear why these crystals had different La contents since the preparation always aimed to obtain $y=1$. Similar problems were encountered in the $\text{Yb}_y\text{Fe}_4\text{Sb}_{12}$ system.^{15,21}

All products are—in contrast to the educts—not at all sensitive to air or moisture. The results presented in the cur-

rent work were obtained on samples of the same batches used in the previous publications.^{9,15} Powder samples were washed in hydrochloric acid in order to remove elemental iron which otherwise would negatively affect magnetization measurements.⁹ Due to the different preparation route this procedure is not necessary for $\text{La}_y\text{Fe}_4\text{Sb}_{12}$ crystals. Physical measurements were performed on single crystals or polycrystalline specimens cut from spark-plasma sintered (SPS) material (92% compaction) as described previously.⁹ Metallographic microstructure photographs and electron-probe microanalysis (wavelength dispersive analysis, Cameca SX100) were done on polished surfaces. The analyses were carried out with elemental Fe and Sb standards together with BaGe_4 for barium, LaPt_2 for lanthanum, and andradite for Ca, respectively. Energy dispersive analysis of the samples was carried out in a Philips XL30 scanning electron microscope. In the SPS samples these investigations revealed only elementary antimony as an impurity phase (about 2 vol %).⁹

B. Crystal structure investigations

Powder x-ray diffraction (XRD) measurements were made using $\text{Cu } K\alpha_1$ radiation ($\lambda=1.54060 \text{ \AA}$) applying Guinier technique with LaB_6 as an internal standard ($a=4.15692 \text{ \AA}$). Low-temperature powder XRD was performed on a Huber Guinier camera with a sample holder incorporated in a closed-cycle helium cryostat. For correct lattice parameter determination, the measurements were performed with silicon powder ($a=5.4311946 \text{ \AA}$) used as an internal standard.²³ Powder neutron diffraction data were taken at the Hahn-Meitner-Institut, Berlin, with instrument E9.

Low-temperature powder synchrotron data of $\text{CaFe}_4\text{Sb}_{12}$ were collected at beamline B2, Hasylab at DESY, Hamburg, in a specially designed cryostat²⁴ between 50 and 300 K. The powder with grain size $<25 \mu\text{m}$ was placed in a quartz capillary with diameter 0.3 mm and mounted inside the cryostat. Radiation with wavelength of 0.49349 \AA was used. Temperature-dependent single-crystal XRD data were collected between 110 and 295 K on a Stoe IPDS system ($\text{Ag } K\alpha$ radiation; $\lambda=0.56086 \text{ \AA}$) and at room temperature on a Rigaku R -axis RAPID diffractometer ($\text{Mo } K\alpha$ radiation 0.71073 \AA). Crystallographic calculations were made with the WINCSD (Ref. 25) and the SHELXL-97 (Ref. 26) program packages.

C. Physical properties

Magnetic properties were measured on a superconducting quantum interference device magnetometer (MPMS XL-7, Quantum Design). Zero-field cooling (measured in warming) and field-cooling runs, and isothermal magnetization loops were performed up to $\mu_0 H=7 \text{ T}$. Additional isothermal magnetization curves up to $\mu_0 H=14 \text{ T}$ were measured by an extraction technique (PPMS, Quantum Design). No demagnetization or diamagnetic core corrections were applied. The pressure dependence of the magnetization was checked in a miniature Cu-Be pressure cell. The superconducting transition temperature of a piece of Pb in the sample space was used to determine the pressure.

Heat capacity was determined by a relaxation method in PPMS instruments with fields up to $\mu_0 H = 14$ T. The estimated inaccuracy of $c_p(T)$ below 100 K is about 1%, above 100 K it increases with T to 2%–4% of $c_p(T)$, depending on the sample's thermal diffusivity and mass.

Electrical resistance was measured with ac ($f = 13.73$ Hz, $I = 32$ mA) on bar-shaped polycrystalline SPS samples or on cut and polished single crystals in a PPMS. When necessary, nominal zero-field data of $\rho(T)$ were measured in $\mu_0 H = 10$ mT in order to suppress the instrumental artifact of MPMS ac-transport data around $T = 30$ K. Transversal magnetoresistance was determined by sweeping the temperature at constant magnetic fields and by isothermal magnetic field sweeps ($0 \text{ T} \rightarrow +9 \text{ T} \rightarrow 0 \text{ T} \rightarrow -9 \text{ T} \rightarrow 0 \text{ T}$) at selected temperatures. For single-crystal samples, the current flow was approximately along a $[100]$ direction, the field along a perpendicular direction. The Hall effect was derived from similar isothermal magnetic field sweeps on the same samples in a five-contact arrangement in a PPMS. The curves $\rho_{xy}(H)$ are in many cases nonlinear and the adjustment for zero ρ_{xy} at $H = 0$ (compensation for the misalignment of the Hall contacts) at room temperature was not stable at lower temperatures, even in paramagnetic samples. The transverse magnetoresistance was found to be small in low fields and hence its contribution to ρ_{xy} at low fields can be neglected. Thus, the Hall coefficient $R_H(T)$ was determined from the slope at low fields for several temperatures. In measurements on ferromagnetically ordered phases the skew scattering strongly influences the results (anomalous Hall effect) so that only the data of $R_H(T)$ above T_C will be considered.

D. Band structure calculations

The electronic structure of $M\text{Fe}_4\text{Sb}_{12}$ ($M = \text{K}, \text{Ca}, \text{La}$) has been calculated using the full-potential nonorthogonal local-orbital calculation scheme (FPLO, version 5.00-19)²⁷ within the local (spin) density approximation [L(S)DA]. In the scalar-relativistic calculations the exchange and correlation potentials of Perdew and Wang²⁸ were used. As the basis set, K ($3s, 3p, 4s, 4p, 3d$), Ca ($3s, 3p, 4s, 4p, 3d$), La ($4s, 4p, 5s, 5p, 5d$), Fe ($3s, 3p, 4s, 4p, 3d$), and Sb ($4s, 4p, 4d, 5s, 5p, 5d$) states were employed. The lower lying states were treated fully relativistically as core states. The K or Ca $3d$ states as well as the Sb $5d$ states were taken into account as polarization states to increase the completeness of the basis set. The treatment of the K or Ca ($3s, 3p$), La ($4s, 4p$), Fe ($3s, 3p$), and Sb ($4s, 4p, 4d$) semicorelike states as valence states was necessary to account for non-negligible core-core overlaps. The spatial extension of the basis orbitals, controlled by a confining potential $(r/r_0)^4$,⁴ was optimized to minimize the total energy.²⁹ In the self-consistent cycle, a k mesh of 396 points in the irreducible part of the Brillouin zone (8000 in the full zone) was used to ensure accurate density of states and band structure information, especially in the region close to the Fermi level. The Fermi surfaces were calculated on a $60 \times 60 \times 60$ grid.

III. RESULTS AND DISCUSSION

A. Crystal structure

In Table I we summarize the relevant crystallographic data and the chemical composition of the compounds inves-

tigated. All compounds crystallize with the $\text{LaFe}_4\text{P}_{12}$ type¹ with a body-centered cubic unit cell. Where single crystals were available XRD analyses of $M\text{Fe}_4\text{Sb}_{12}$ yielded also occupancy data for the $2a$ position of the cation and refined positional parameters of the Sb atoms on the $24g$ site. The cation resides inside a large distorted icosahedral cage in the antimony-iron framework. Iron atoms are located on an $8c$ position and are octahedrally coordinated by six Sb atoms.

With the values in Table I the obtained atomic displacement parameters (ADPs) (U_{iso}) can be compared with the relevant static parameter of the structure, namely, the radius of the icosahedral voids formed by the Sb atoms. These radii were calculated in the same way as previously outlined by Nolas *et al.*³³ The distance from the center of the void to any of the 12 surrounding Sb atoms minus the radius of the Sb atom r_{Sb} is regarded as the void radius. r_{Sb} is defined as half of the average Sb-Sb separation in the individual skutterudite. For the cations ionic radii compiled by Shannon³⁴ were used. Theoretical chemical bonding studies^{9,35} indicate a complete charge transfer from the cation to the polyanionic host. Therefore, we can use the ionic model as a first approximation.

Comparing the void radii with the cation radii it can be easily seen that the latter are considerably smaller. This structural peculiarity can be observed in all skutterudite compounds with a transition-metal-antimony-based framework structure and, thus, allows significantly larger vibrations of the cations as compared to the vibrations of the atoms constituting the host. These vibrations are visible in the mean square displacement of the cation about its equilibrium position which is experimentally available in diffraction experiments from the ADPs. Indeed the ADPs of the cations are significantly larger and strongly temperature dependent compared to the atoms of the polyanion (Fig. 1, cf. reviews in Refs. 2 and 7).

These observations have been paraphrased in literature as a “rattling” motion of an atom in an oversized cage which is only loosely bonded to the cage-forming atoms. While the term “rattling” illustrates the large ADPs in a general metaphorical sense rather well, it can also suggest an anharmonic atomic potential well which evidence can hardly be provided from room-temperature ADPs only. Sales *et al.*^{32,36} recently discussed these implications in detail and showed that the rather high room-temperature ADPs of filler atoms observed in compounds adopting clathrate and skutterudite structures can be correlated with their low lattice thermal conductivity and with the temperature dependence of their heat capacity at low temperatures, provided the “rattler” can be treated as an Einstein oscillator. This structure-property relationship is limited by the liability of ADPs to shortcomings in the actual diffraction measurements (absorption problems applying x rays and static disorder). Moreover, ADPs provide no information about correlations with the motions of other atoms.³⁶ It is therefore necessary for this model to consider the surrounding cage of Sb atoms as rather rigid and not significantly responding to the vibrations of the cations.

Assuming independent vibrations of the fillers, harmonic potential wells, and rigid cage walls, Einstein temperatures Θ_E^{ADP} can be calculated from ADPs applying formula (2) from Ref. 37. The Θ_E^{ADP} (including some literature data)

TABLE I. Cubic lattice parameters a and atomic displacement parameters (ADPs) (U_{iso}) for $M\text{Fe}_4\text{Sb}_{12}$ filled skutterudites at temperature T . Structure type: $\text{LaFe}_4\text{P}_{12}$. Space group: $Im\bar{3}$, $Z=2$. r_{cage} radii of the icosahedral void; Θ_E^{ADP} Einstein temperature derived from the ADPs; Θ_E^{C} Einstein temperature from specific heat data; $\text{RT} \approx 293$ K.

| M | Composition | a (Å) | r_{cage} (Å) | $r_{\text{cage}}/r_{\text{ionic}}$ | U_{iso} (Å ²) | T (K) | Θ_E^{ADP} (K) | Θ_E^{C} (K) | |
|------------------|---|---|-----------------------|------------------------------------|------------------------------------|-----------|-----------------------------|---------------------------|-----|
| Na ⁸ | Na _{0.95(1)} Fe _{4.08(1)} Sb _{11.92(1)} | 9.1767(5) | 1.9401 | 1.40 | 0.0220(3) | RT | 170 | 81 | |
| | | 9.1759(8) ^a | | | 0.041(5) | 300 | 125 | | |
| | Na _{0.97(3)} Fe ₄ Sb ₁₂ ^b | | | | 0.0221(3) | | | 170 | |
| | | NaFe ₄ Sb ₁₂ | | | | 0.0242(1) | | | 162 |
| Ca ^c | Ca _{0.91(1)} Fe _{4.02(2)} Sb _{12.05(3)} | 9.1631(4) | 1.9344 | 1.44 | 0.0233(6) | RT | 125 | 88 | |
| | | | | | 0.0212(1) | | 130 | | |
| | Ca _{0.87(1)} Fe ₄ Sb ₁₂ ^b | | | | 0.0274(3) | | | 114 | |
| | | CaFe ₄ Sb ₁₂ | | | | 0.0258(2) | | | 118 |
| Sr ^c | SrFe ₄ Sb ₁₂ | 9.1810(3) | 1.9548 | 1.36 | 0.0191(6) | RT | 93 | 93 | |
| | Sr _{0.83(1)} Fe ₄ Sb ₁₂ ^b | | | | 0.0112(9) | | | 121 | |
| | Sr _{0.93(1)} Fe ₄ Sb ₁₂ ^d | 9.1812(6) | | | 0.0128(3) | | | 113 | |
| Ba ^c | Ba _{0.96(2)} Fe _{4.03(2)} Sb _{12.03(3)} | 9.2058(2) | 1.9880 | 1.23 | 0.0053(3) | RT | 140 | 104 | |
| | | | | | 0.0064(1) | | 128 | | |
| | BaFe ₄ Sb ₁₂ | | | | 0.0066(3) | | | 126 | |
| | | Ba _{0.84(1)} Fe ₄ Sb ₁₂ ^e | | | | 0.0103(3) | | | 100 |
| La | La _{0.87(1)} Fe _{4.08(1)} Sb _{12.1(1)} | 9.1454(5) | 1.9329 | 1.42 | 0.0167(5) | RT | 79 | 77 | |
| | | | | | 0.0184(6) | | 75 | | |
| | La _{0.91(1)} Fe ₄ Sb ₁₂ ^b | | | | 0.0220(6) | | | 68 | |
| | | LaFe ₄ Sb ₁₂ | | | | 0.013(1) | | | 88 |
| Yb ¹⁵ | Yb _{0.97(1)} Fe _{3.98(2)} Sb _{12.1(2)} | 9.1586(5) | 1.9288 | | 0.0215(2) | RT | 61 | 62 | |
| | | | | | 0.0252(4) | | 57 | | |
| | YbFe ₄ Sb ₁₂ ^f | | | | 0.0196(9) | | | 65 | |

^aFrom neutron powder diffraction.

^bOccupancies refined from single crystal XRD.

^cRefined Sb ($0, y, z$) positions at RT: CaFe₄Sb₁₂ [0, 0.15958(2), 0.33667(2)]; SrFe₄Sb₁₂ [0, 0.16003(5), 0.33797(5)]; BaFe₄Sb₁₂ [0, 0.16134(4), 0.34021(4)].

^dReference 30.

^eReference 31.

^fReference 32.

might now be compared with values Θ_E^{C} derived from specific heat data (see Sec. III C and Table I).

Regarding heavy cations, Θ_E^{ADP} values match Θ_E^{C} values amazingly well. There is, however, some discrepancy concerning BaFe₄Sb₁₂, where Θ_E^{ADP} significantly deviates from the value derived from c_p data. Calculation of Θ_E^{ADP} based on ADP values derived by Stetson *et al.*³¹ gives a better agreement despite the fact that their crystals were significantly off-stoichiometric. A more puzzling phenomenon is revealed comparing the values of the Ba-containing compound with La_yFe₄Sb₁₂, where the masses of the cations are the same within less than 2 amu but the Θ_E^{ADP} as well as Θ_E^{C} significantly are at variance. Larger values for La_yFe₄Sb₁₂ can be understood taking into account the larger $r_{\text{cage}}/r_{\text{ion}}$ value, i.e., the La ion has more freedom in (thermal) motion. Discrepancies increase if we compare the Θ_E found for skutterudites with lighter cations. For CaFe₄Sb₁₂ and SrFe₄Sb₁₂ single-

crystal data from literature reveal similar behavior like the analysis of our crystals, namely, significantly higher Θ_E^{ADP} values compared with Θ_E^{C} . On the other hand, Θ_E^{C} for KFe₄Sb₁₂ and CaFe₄Sb₁₂ with very similar cation masses are more or less the same. Due to the lack of KFe₄Sb₁₂ single crystals no ADP values are available.

Another observation can be made comparing data of CaFe₄Sb₁₂ and YbFe₄Sb₁₂ which, according to recent band structure calculations and physical properties measurements,^{15,19} have very similar electronic properties and unit cell dimensions. Here, for a first approximation, scaling of the Einstein temperatures with filler mass (Yb being about four times heavier than Ca) is expected. Within the harmonic oscillator model the force constant k can be expressed by $k = m(k_B\Theta_E/\hbar)$.² A ratio $k_{\text{Ca}}/k_{\text{Yb}} \approx 0.46$ is found which would indicate a significant difference of the potential wells for the cation vibrations. If we follow the same line of

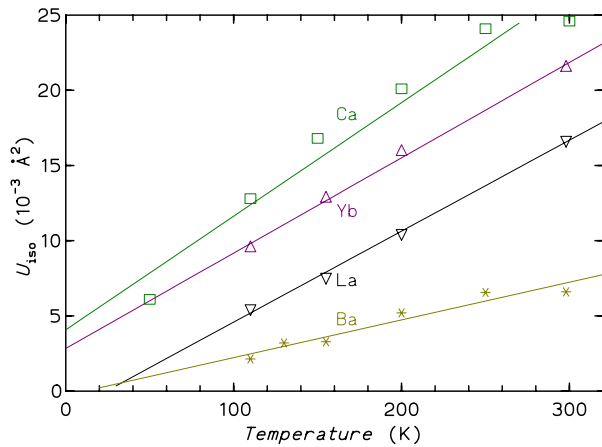


FIG. 1. (Color online) Temperature dependence of isotropic displacement parameters of the cations in $M\text{Fe}_4\text{Sb}_{12}$ ($M = \text{Ca}, \text{Ba}, \text{La}_{0.87}, \text{Yb}_{0.97}$). The lines are linear fits to the data.

arguments for Ba and La filled skutterudites we have to conclude that the force constant k_{Ba} is about 1.8 times larger than k_{La} indicating a deeper potential. Also the slopes dU_{iso}/dT for the two compounds [fits in Fig. 1: Ba $2.6(4) \text{ \AA}^2/\text{K}$, La $6.0(2) \text{ \AA}^2/\text{K}$] differ by roughly this factor.

On the other hand, the significant increase of Θ_E^C from Ca to Sr and Ba cannot be understood at all by the simple assumptions of a harmonic oscillator model (decreasing vibration frequencies with increasing atomic masses). There, the trend should be exactly the other way round. Only if in the sequence $k_{\text{Ba}} > k_{\text{Sr}} > k_{\text{Ca}}$ the values of k increase stronger than the atomic masses, the Einstein temperatures will increase. We, however, observe a decrease in the ratio $r_{\text{cage}}/r_{\text{ionic}}$ when moving from Ca to Ba, thus tightening the confinement of the cations. This is in qualitative agreement with the observation of a larger slope dU_{iso}/dT for the Ca compound compared with the Ba homolog (see Fig. 1).

For $\text{NaFe}_4\text{Sb}_{12}$, the skutterudite compound with the lightest cation to date, the disagreement of the Θ_E^{ADP} and Θ_E^C values is maximal. Much higher ADPs should be observed. From this analysis it can be concluded that Θ_E^{ADP} values match Θ_E^C values only for heavy fillers, e.g., the rare-earth metals, in line with previous investigations of Sales *et al.*^{32,36} Severe discrepancies are immediately encountered for skutterudites with lighter fillers. These findings thus suggest significant differences in the cation potentials as well as hybridization effects which cannot be treated by the simplistic harmonic oscillator model.

B. Paramagnetic moment of the $[\text{Fe}_4\text{Sb}_{12}]$ polyanion

The magnetic properties of $M\text{Fe}_4\text{Sb}_{12}$ skutterudites depend on the nonmagnetic filler ion M . Figure 2 summarizes the inverse magnetic susceptibility data $\chi(T)$ for the investigated purified $M\text{Fe}_4\text{Sb}_{12}$ samples. It can be seen that for high temperatures ($T > 100\text{--}150 \text{ K}$) $\chi(T)$ is well described by a Curie–Weiss law. To obtain this picture it is imperative to use samples with very low levels of ferromagnetic (i.e., metallic iron) impurities in measurements at high external magnetic

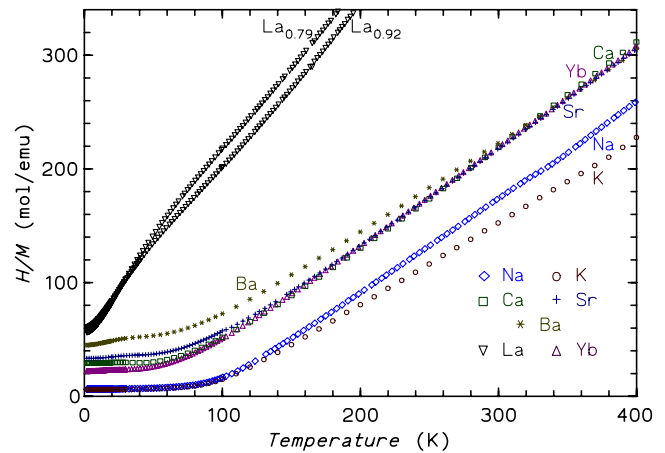


FIG. 2. (Color online) Inverse magnetic susceptibility H/M of filled skutterudites $M\text{Fe}_4\text{Sb}_{12}$ ($M = \text{Na}, \text{K}, \text{Ca}, \text{Sr}, \text{Ba}, \text{La}_{0.79}, \text{Yb}_{0.97}$) for high external fields and corrected for ferromagnetic impurities.

fields (see discussion in Ref. 9). $\text{NaFe}_4\text{Sb}_{12}$ and $\text{KFe}_4\text{Sb}_{12}$ order ferromagnetically at $\approx 80 \text{ K}$ while the other compounds stay paramagnetic down to 1.8 K . The paramagnetic effective moments $\mu_{\text{eff}}/\text{Fe atom}$ are $1.5\text{--}1.7\mu_B$ with $\Theta_P \approx +85 \text{ K} \approx T_C$ for the compounds with monovalent $M = \text{Na}, \text{K}$ ions and smaller positive Θ_P for compounds with divalent M ions (Ca: $+45 \text{ K}$, Sr: $+41 \text{ K}$, Ba: $+20 \text{ K}$, $\text{Yb}_{0.95}$: $+45 \text{ K}$).^{9,15}

For the weaker paramagnetic $\text{La}_y\text{Fe}_4\text{Sb}_{12}$ a negative temperature-independent contribution χ_0 becomes visible at high temperatures. While fits with a modified Curie–Weiss model result in $\chi_0 \approx -500 \times 10^{-6} \text{ emu mol}^{-1}$ for both compositions we preferred to fix χ_0 to the sum of the diamagnetic core contributions ($\chi_{\text{dia}} = -240 \times 10^{-6} \text{ emu mol}^{-1}$).³⁸ Fits yield smaller values of $\mu_{\text{eff}}/\text{Fe atom} = 1.23\mu_B$ ($y = 0.79$) and $y = 0.92$) and clearly negative $\Theta_P = -56 \text{ K}$ ($y = 0.79$) and -44 K ($y = 0.92$). These parameters depend significantly on the choice of χ_0 and of the temperature range of the fit. The parameters are in fair agreement with those of Viennois *et al.*³⁹ $\mu_{\text{eff}}/\text{Fe atom} = 1.13$ or $1.18\mu_B$, $\Theta_P = -42$ or -55 K , albeit with $\chi_0 = 0$. The $\text{La}_y\text{Fe}_4\text{Sb}_{12}$ crystals as well as polycrystalline materials do not show ferromagnetic impurities.

Obviously, the values of μ_{eff} cannot be explained by assuming Fe^{2+} and Fe^{3+} ions with localized moments. The occurrence of ferromagnetic order with small moments of $0.25\text{--}0.28\mu_B/\text{Fe atom}$ (remanence) proves that the Na, K, and Tl (Ref. 10) compounds are itinerant magnetic systems. The Curie–Weiss law observed for all seven compounds, the saturation of M/H for $\mu_0 H \geq 1 \text{ T}$ at low temperatures, and the hump around $T = \Theta_P$ in the paramagnetic compounds¹⁵ thus can be understood as fingerprints of strong spin fluctuations. According to Moriya,⁴⁰ in the nonordering compounds the Weiss temperature should be taken as the typical energy scale of the spin fluctuations.

When increasing the cation charge from $1+$ to $2+$, μ_{eff} decreases only slightly (by $\approx 0.1\mu_B$) but Θ_P reduces to half the value of the compounds which order magnetically. Also, there is a trend of decreasing Θ_P in the series Ca/Yb, Sr, Ba. The most influential factor is presumably the lattice volume, which increases in this sequence of cations. This is fully consistent with the ordered moment values obtained from

fixed spin moment calculations:¹⁴ The calculated gain in energy and the ordered moment for the ferromagnetic solution decrease in the same sequence Yb, Ca (very little less than for Yb), Sr, Ba.

Even for La a tiny energy gain is calculated for the ferromagnetic state; however, since the experimental value of the Weiss temperature Θ_p is clearly negative a more favorable antiferromagnetic solution might be found. In a recent NMR investigation by Gippius *et al.*⁴¹ it was concluded from a typical $T^{-1/2}$ dependence of the spin relaxation time $1/T_1$ that in $\text{La}_y\text{Fe}_4\text{Sb}_{12}$ antiferromagnetic spin fluctuations are dominating. There are, however, also indications for the presence of ferromagnetic spin fluctuations.^{39,42,43}

The Curie temperature of polycrystalline $\text{NaFe}_4\text{Sb}_{12}$ increases approximately linearly with pressure (at 1.42 GPa by +4.2 K) with a rate of ≈ 3 K/GPa, i.e., by +3.7%/GPa. Also, an increase of the coercive field at 1.8 K by $\approx 20\%$ and upturn of $M(H)$ for temperatures below ≈ 15 K was observed at low temperatures and maximum applied pressure (1.42 GPa). In electronic structure calculations within the LSDA the magnetic moment is suppressed with decreasing lattice parameter (i.e., applying pressure). As a consequence T_C should decrease with pressure. A positive dT_C/dp indicates that the damping of the spin fluctuations by application of pressure is more effective than the reduction of the mean-field moment. One may speculate that application of pressure might drive the paramagnetic compounds with divalent cations toward ferromagnetic ordering. Actually, in $\text{CaFe}_4\text{Sb}_{12}$ a similar increase of $M(H)$ for temperatures below that of the hump (i.e., below $\approx \Theta_p$) could be found. However, for small pressures up to 1.2 GPa and various fields no ferromagnetism could be induced in $\text{CaFe}_4\text{Sb}_{12}$.

C. Specific heat capacity

The molar heat capacity $c_p(T)$ of all seven compounds is displayed in Fig. 3. For temperatures well above 100 K the values of $c_p(T)$ for $M=\text{Na}, \text{K}, \text{Ca},$ and $\text{La}_{0.92}$ are identical within the estimated accuracy of the measurements, only for $M=\text{Ba}$ $c_p(T)$ is significantly larger. For this Ba sample (a conventional sinter with low compaction) the significantly higher c_p (+2%–3%) above 200 K is probably due to the low thermal diffusivity of the pellet and the connected thermal radiation losses. The data for the compounds with $M=\text{Na}, \text{K}$ display a small second-order anomaly at 81 K (transition midpoint for the Na sample) and 80 K (K), respectively, with widths less than 1% of T_C , in good agreement with the Curie temperatures determined by magnetization measurements.⁹

Figure 4 displays the specific heat below 14 K in the c_p/T vs T^2 representation. It is already obvious that the electronic term γT for the compounds with Na, K, Ca, Sr, and Ba is of the same size (100–120 $\text{mJ mol}^{-1} \text{K}^{-1}$). Only $\text{La}_y\text{Fe}_4\text{Sb}_{12}$ samples show clearly a large value (≈ 200 $\text{mJ mol}^{-1} \text{K}^{-2}$). In order to make the differences in the specific heats visible one has to subtract $c_p(T)$ of a suitable reference compound. Since the nonfilled FeSb_3 skutterudite does not exist in bulk form we have chosen the specific heat of $\text{CaFe}_4\text{Sb}_{12}$ as the reference.

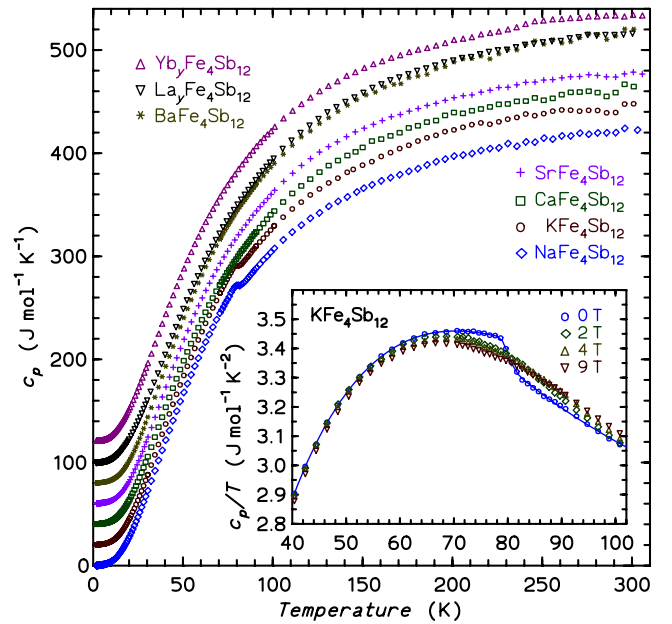


FIG. 3. (Color online) Specific heat of filled skutterudites $M\text{Fe}_4\text{Sb}_{12}$ ($M=\text{Na}, \text{K}, \text{Ca}, \text{Sr}, \text{Ba}, \text{La}_{0.92}, \text{Yb}_{0.97}$) (main panel). Curves have been shifted by 20 units each. The inset shows the field dependence of the specific heat of $\text{KFe}_4\text{Sb}_{12}$ near the ferromagnetic transition.

Figure 5 shows the differences $\Delta c_p(T)/T$ for all investigated compounds to $c_p(T)$ of the Ca compound (actually, to a spline fitted to the $\text{CaFe}_4\text{Sb}_{12}$ data). As already established above, the electronic terms of the Na, K, Ca, Sr, and Ba compounds are almost identical, viz., $\Delta c_p/T \rightarrow 0$ for $T \rightarrow 0$. For the Yb compound an upturn of $\Delta c_p(T)$ and a small lambda peak are visible which is due to ≈ 0.5 mol % of Yb_2O_3 , which orders antiferromagnetically around 2.3 K.²⁰ For a comprehensive discussion of this problem we refer to Refs. 15 and 22 and the recent paper by Ikeno *et al.*²¹ The value of γ of $\text{YbFe}_4\text{Sb}_{12}$ seems to be only slightly larger than that of $\text{CaFe}_4\text{Sb}_{12}$, consistent with band structure

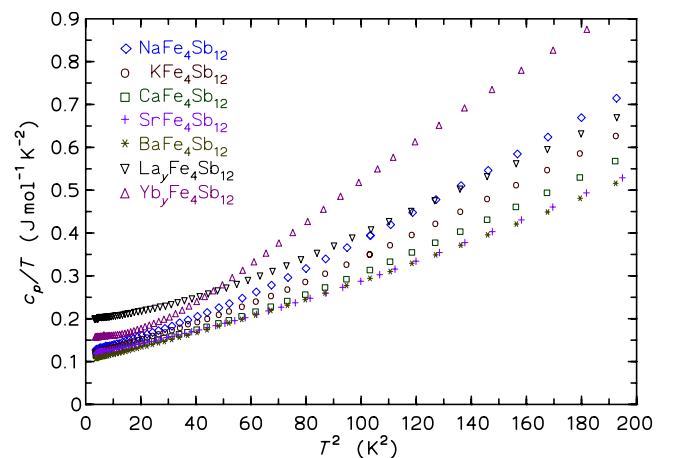


FIG. 4. (Color online) Specific heat capacity of filled skutterudites $M\text{Fe}_4\text{Sb}_{12}$ ($M=\text{Na}, \text{K}, \text{Ca}, \text{Sr}, \text{Ba}, \text{La}_{0.79}, \text{Yb}_{0.95}$) below 14 K in a c_p/T vs T^2 representation.

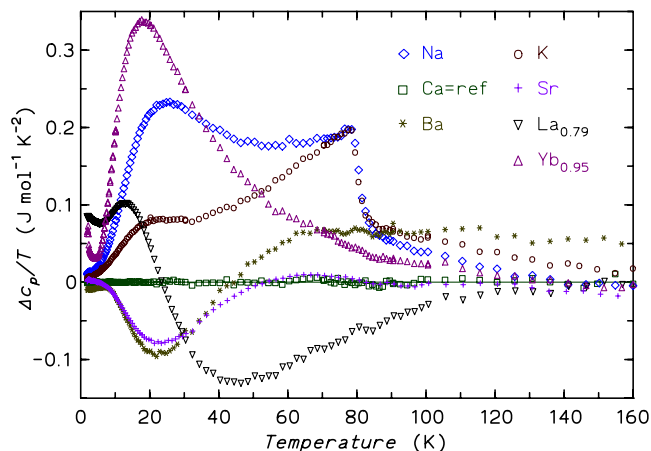


FIG. 5. (Color online) Difference of the specific heats $\Delta c_p/T$ of filled skutterudites $M\text{Fe}_4\text{Sb}_{12}$ ($M=\text{Na}, \text{K}, \text{Ca}, \text{Sr}, \text{Ba}, \text{La}_{0.79}, \text{Yb}_{0.95}$) to a smooth fit of $c_p(T)$ of $\text{CaFe}_4\text{Sb}_{12}$.

calculations.¹⁵ For the compounds with divalent cations (Ca, Sr, Ba, Yb) the Sommerfeld-Wilson ratio $R_W = \pi^2 k_B^2 \chi / 3 \mu_B^2 \gamma$ (with the low-temperature susceptibility χ) is very large (≈ 24 for $\text{Yb}_y\text{Fe}_4\text{Sb}_{12}$ and $\text{CaFe}_4\text{Sb}_{12}$),¹⁵ indicating that they

are close to ferromagnetic ordering. Actually, Yoshii *et al.*⁴⁴ reported that for $T \leq 50$ K Ca, Sr, and even $\text{BaFe}_4\text{Sb}_{12}$ exhibit itinerant electron metamagnetism and display broad metamagnetic transitions to a ferromagnetically ordered state (for $\text{CaFe}_4\text{Sb}_{12}$ above $\mu_0 H = 13$ T).

Values of γ obtained from fits of a simple model $c_p(T) = \gamma T + \beta T^3 + \delta T^5$ for $T < 7$ K including the electronic term and the Debye T^3 and T^5 terms^{47–49} are given in Table II. For $\text{La}_y\text{Fe}_4\text{Sb}_{12}$ an additional field-dependent SF contribution to $c_p(T)$ at low temperatures is observed. An analysis of $c_p(T)$ from zero-field data only leads to unrealistic results. A deconvolution of $c_p(T, H)$ data of $\text{La}_y\text{Fe}_4\text{Sb}_{12}$ into its contributions is presented in Sec. III E.

D. Low-lying phonon term

The large differences in $c_p(T)$ of the filled skutterudites at medium temperatures cannot be explained by electronic or magnetic contributions but are of phononic origin. In a simplistic model, the thermal excitations of the cation in its relatively large icosahedral Sb environment lead to a low-lying phonon mode. In a first approximation the phonon can be described by an Einstein term (characteristic temperature

TABLE II. Parameters resulting from fits of the zero-field specific heat $c_p(T)$ to a simple ($T < 7$ K; Debye+electronic term) model (first line for each compound) and to Eq. (1) including an additional Einstein term ($T^2 < 200$ K², second and third lines for each compound). $R = 8.314\,472$ J mol⁻¹ is the molar gas constant. Θ_D was calculated from β with 16 atoms of the $[\text{Fe}_4\text{Sb}_{12}]$ polyanion, but for 17 atoms for the simple model. Numerical-only inaccuracy of the last digits is given in parentheses. For La compounds see Sec. III E.

| Compound | Electronic term γ (mJ mol ⁻¹ K ⁻²) | T^3 and T^5 Debye terms | | | Einstein term | |
|--|--|--|-------------------|--|---------------|-------------------|
| | | β (mJ mol ⁻¹ K ⁻⁴) | Θ_D (K) | δ ($\mu\text{J mol}^{-1}$ K ⁻⁶) | $\epsilon/3R$ | Θ_E (K) |
| $\text{NaFe}_4\text{Sb}_{12}$ (simple) | 122.0(0.4) | 1.625(36) | 273 | 10.7(7) | | |
| $\text{Na}[\text{Fe}_4\text{Sb}_{12}]$ | 116.4(0.6) | 2.172(18) | 243 | 0.12(5) | 1.00 | 81.6(0.4) |
| | 116.2(0.6) | 2.182(18) | 243 | | 1.02(1) | 81.8(0.4) |
| $\text{KFe}_4\text{Sb}_{12}$ (simple) | 116.3(0.5) | 1.655(43) | 271 | 5.5(8) | | |
| $\text{K}[\text{Fe}_4\text{Sb}_{12}]$ | 113.1(0.4) | 1.949(11) | 252 | ≈ 0 | 1.00 | 86.4(0.3) |
| | 113.2(0.4) | 1.944(12) | 252 | | 0.99(1) | 86.1(0.5) |
| $\text{CaFe}_4\text{Sb}_{12}$ (simple) | 112.4(0.4) | 1.325(30) | 292 | 5.5(5) | | |
| $\text{Ca}[\text{Fe}_4\text{Sb}_{12}]$ | 109.1(0.4) | 1.614(10) | 268 | 0.53(5) | 1.00 | 87.8(0.4) |
| | 108.5(0.5) | 1.651(13) | 266 | | 1.15(2) | 88.8(0.5) |
| $\text{SrFe}_4\text{Sb}_{12}$ (simple) | 115.7(0.3) | 1.229(23) | 300 | 4.5(4) | | |
| $\text{Sr}[\text{Fe}_4\text{Sb}_{12}]^a$ | 111.8(0.3) | 1.491(07) | 275 | 0.59(5) | 1.00 | 92.6(0.4) |
| | 111.2(0.4) | 1.535(10) | 273 | | 1.19(2) | 93.6(0.6) |
| $\text{BaFe}_4\text{Sb}_{12}$ (simple) | 102.4(0.3) | 1.418(25) | 286 | 5.2(4) | | |
| $\text{Ba}[\text{Fe}_4\text{Sb}_{12}]$ | 98.1(0.4) | 1.733(11) | 262 | 0.78(19) | 1.00 | 104.2(2.0) |
| | 97.8(0.6) | 1.773(14) | 260 | | 1.18(8) | 101.4(1.6) |
| $\text{YbFe}_4\text{Sb}_{12}$ (simple) | 141.2(4.2) | 0.647(226) | 364 | 37.0(30) | | |
| $\text{Yb}_y[\text{Fe}_4\text{Sb}_{12}]^b$ | 138.1(1.1) | 1.808(25) | 258 | ≈ 0 | 0.95 | 63.0(0.3) |
| | 116.7(1.3) | 2.388(34) | 235 | | 0.70(2) | 61.8(1.2) |

^aRange of fit [3 K, 14.1 K].

^bCation filling level $y=0.95$; range of fit [5 K, 14.1 K].

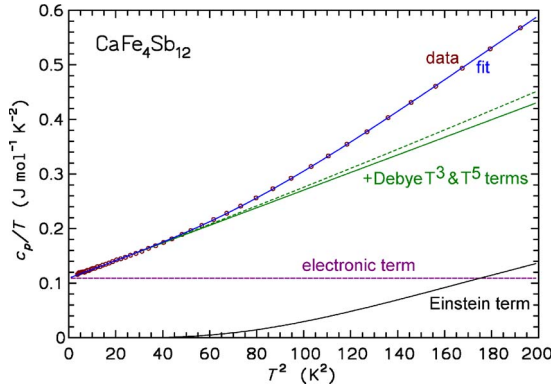


FIG. 6. (Color online) Specific heat of $\text{CaFe}_4\text{Sb}_{12}$ below 14 K. The lines give the contributions of the individual terms of the fit in Eq. (1).

$\Theta_E = \hbar\omega_E/k_B$) centering the mode in the phonon density of states. It has to be mentioned that the Einstein model applies equally well to an optical phonon mode (with low dispersion) as to an ensemble of independent localized (rattling) oscillators.

A model for the specific heat involving an Einstein mode has previously been applied to rare-earth^{15,45} or thallium⁴⁶ ions in skutterudites. Similar to these previous studies we interpret here the specific heat as a combination of an Einstein mode with a Debye model (Debye temperature Θ_D) for the remaining 16 atoms of the polyanion $[\text{Fe}_4\text{Sb}_{12}]$. $c_p(T)$ at low T is fitted by

$$c_p(T) = \gamma T + \beta T^3 + \delta T^5 + \epsilon \mathcal{E}(T/\Theta_E), \quad (1)$$

where β contains the Debye temperature Θ_D and \mathcal{E} is the Einstein function.^{47,48} This model is not expected to work at higher temperatures where optical (Einstein) terms of the host need to be taken into account and the Debye approximation fails.

There are two kind of reasonable fits: Firstly, as in Ref. 15, the coefficient ϵ of the Einstein term can be fixed to the value $3Ry$ ($R = k_B N_A$) with the filling level y as determined by chemical analysis. Secondly, ϵ can be allowed to vary. An interval 1.8–14.1 K was chosen for fits to $c_p(T)$ at zero field, except for $\text{Yb}_y\text{Fe}_4\text{Sb}_{12}$ where the Yb_2O_3 impurity hampers the analysis for $T < 5$ K.

It is observed that the fits where both δ and ϵ are allowed to vary result in too large δ and very small ϵ with a large nonsystematic scatter of these parameters. Obviously, a strong numerical anticorrelation of δ with ϵ exists and, thus, the results of these fits are not reliable. Therefore the extra Debye T^5 term ($\delta := 0$) was neglected when ϵ was varied, which should be a reasonable approximation for $T/\Theta_D < 0.05$.^{47–49}

Results of the fits are given in Table II. For the first kind of fits it is observed that δ is indeed much smaller than the Einstein contribution ($\delta < 1 \mu\text{J mol}^{-1} \text{K}^{-6}$), proving that it can be neglected for fits in the chosen temperature range. As a typical example, the various contributions are shown for the $\text{CaFe}_4\text{Sb}_{12}$ data in Fig. 6. The second kind of fits with variable ϵ (and $\delta = 0$) result in parameters which are close to

those from the first kind. Except for the fits on the Yb compound data, the fitted parameters ϵ deviate only by $\pm 19\%$ from the value $3Ry$ expected in this simple model. For the light cations $M = \text{Na}, \text{K}$ the agreement is excellent while for $M = \text{Ca}, \text{Sr}$, and Ba somewhat larger values of ϵ are found. Only for $M = \text{Yb}$ is a significantly smaller ϵ obtained. The impurity hampers a more precise determination of γ , Θ_D , and Θ_E for $\text{Yb}_y\text{Fe}_4\text{Sb}_{12}$.^{15,21}

The zero-field electronic terms for the Na, K, Ca, Sr, and Ba compounds range from 98 to 116 $\text{mJ mol}^{-1} \text{K}^{-1}$ and also $\text{Yb}_y\text{Fe}_4\text{Sb}_{12}$ shows a value only slightly larger. The γ values for the compounds with monovalent cations are in excellent agreement with the “bare” γ_0 derived from the electronic density of states (DOS) (cf. Fig. 10) at E_F (Na: 107 $\text{mJ mol}^{-1} \text{K}^{-1}$, K: 112 $\text{mJ mol}^{-1} \text{K}^{-1}$).^{9,14} For $\text{CaFe}_4\text{Sb}_{12}$ and $\text{YbFe}_4\text{Sb}_{12}$ lower values of γ_0 are calculated (Ca and Yb: $\approx 75 \text{ mJ mol}^{-1} \text{K}^{-1}$) indicating only a small renormalization, consistent with the observation of ferromagnetic spin fluctuations.¹⁵ The homolog with the heavier group 8 elements Ru and Os ($M = \text{Ca}, \text{Sr}, \text{Ba}, \text{La}$) display lower values of γ ($\leq 45 \text{ mJ mol}^{-1} \text{K}^{-2}$) suggesting that only in the Fe compounds the large DOS at E_F leads to such large γ values.¹⁸

The Debye temperature Θ_D (value for $T \rightarrow 0$) increases with the charge of the cation from 243 K (Na) to 267 K (Ca) indicating that the covalent bonding within the $[\text{Fe}_4\text{Sb}_{12}]$ polyanion structure is getting stronger with increased charge transferred to it from the cation. A slight decrease of Θ_D with increasing atomic mass of the cation is observed for the divalent cations Ca, Sr, Ba, and Yb. This might indicate a weak coupling of the filler vibrations to the host lattice acoustic phonon modes, i.e., the two phonon systems cannot be treated as totally independent, even at low temperatures. As concluded from fits with fixed ϵ the Debye T^5 coefficient δ is typically below $1 \mu\text{J mol}^{-1} \text{K}^{-6}$ (less than 0.1% of the value of β). With the simple fits this Debye T^5 contribution is strongly overestimated due to the presence of the Einstein term.

The obtained Einstein temperatures Θ_E are between 62 and 104 K. The heavy Yb ion has the lowest Θ_E among the investigated compounds and only the very heavy Tl^{1+} ion in $\text{Tl}_y\text{Co}_{4-x}\text{Fe}_x\text{Sb}_{12}$ ($y \leq 0.8$)⁴⁶ and in the very recently reported skutterudite compound $\text{TlFe}_4\text{Sb}_{12}$ (Ref. 10) displays a lower-lying mode ($\Theta_E \approx 53$ K). The values of Θ_E can be compared with those derived from ADPs from diffraction investigations (see Table I and discussion in Sec. III A), inelastic neutron scattering, extended x-ray absorption fine structure (EXAFS), or nuclear inelastic scattering investigations. For $M = \text{Na}, \text{K}, \text{Ca}, \text{Sr}, \text{Ba}$ ADP values are available. For $M = \text{Yb}$ the values of Cao *et al.*⁵⁰ from EXAFS are 72 and 79 K, respectively, in fair agreement with our results (62 K).

A remarkable result is the fact that the fitted ϵ is significantly lower than $3Ry$ for the heavier cations La (see below), Yb, and especially Tl^{10} and somewhat larger than this value for Ca, Sr, and Ba. The significantly lower ϵ for $\text{Yb}_y\text{Fe}_4\text{Sb}_{12}$ ($\text{TlFe}_4\text{Sb}_{12}$) (Ref. 10) suggests that only 70% (64%)¹⁰ of the spectral weight of the cation vibrations are concentrated in the lowest-lying peak of the phonon density of states and that the remaining weight is dispersed over a wider energy range or contained in peaks at higher energies. Values of ϵ larger

than $3R\gamma$ cannot be understood within the simple model either. They may hint to a contribution of antimony cage atom vibrations to the low-energy phonon mode in the compounds with light cations. The presence of such contributions is reasonable since these cations are lighter or of similar mass than antimony. On the other hand, for heavy cations as Yb or Tl a much weaker coupling between the cation and cage atom vibrations is expected.

For $\text{Eu}_y\text{Fe}_4\text{Sb}_{12}$ the partial phonon DOS for Eu and Fe atoms was determined by Long *et al.*⁵¹ by nuclear inelastic scattering. For the (Mössbauer-active) cation Eu^{2+} in total three peaks were observed at 7.3(1), 12.0(4), and 17.8(5) meV with areas of 3.4(2), 1.1(2), and 0.5(1), in agreement with previous calculations of the partial La phonon DOS in $\text{LaFe}_4\text{Sb}_{12}$.^{52,53} The two higher-energy peaks are in the DOS region of the Sb vibrations while the major peaks of the Fe vibrations are found between 25 and 35 meV. The relative spectral weight of the lowest-lying cation vibration peak is only 68% of the total. A similar splitting of cation phonon DOS can be expected for skutterudites with other heavy cations. Thus, the spectral weight (ϵ) of the Einstein term in the specific heat should be lower than $3R\gamma$. There is actually good agreement of the spectroscopic results on $\text{Eu}_y\text{Fe}_4\text{Sb}_{12}$ (Ref. 51) (spectral weight 68%) with our findings from specific heat (70% or 64% of $3R$). Fits to specific heat data of $\text{Eu}_y\text{Fe}_4\text{Sb}_{12}$ crystals with the model in Eq. (1) fail to give reliable values of ϵ and Θ_E .⁵⁴ This is due to the magnetic contribution of the ordered Eu^{2+} sublattice.⁵⁵ For the skutterudite compounds covered by the present work, data from inelastic neutron scattering investigations and *ab initio* phonon DOS calculations corroborate the above picture.⁵⁶

Recently, also direct indications for a significant coupling of the Sb vibrations to those of the cation have been observed in ^{121}Sb nuclear inelastic scattering data.⁵⁷ All these facts imply a hybridization of the cation vibrations to the host vibrations, namely, to the Sb atoms forming the cavity, even for heavy cations. For heavy cations this coupling has already been discussed for $\text{TlFe}_4\text{Sb}_{12}$.¹⁰ For light cations the hybridization is expected to be much stronger. Thus, the fact that the fits to $c_p(T)$ for compounds with light cations yield values of ϵ close to or slightly larger than $3R\gamma$ might be just accidental.

E. Field dependence of specific heat: $\text{La}_y\text{Fe}_4\text{Sb}_{12}$

Figure 7 shows the field dependence of $c_p(T)$ for four of the investigated skutterudites. While there is a small decrease of γ detectable for the ferromagnetically ordered phases, no change of γ with H is resolved for the nearly ferromagnetic compounds. For paramagnetic compounds with SFs a sizable field dependence of the nonphononic contributions to $c_p(T)$ was frequently observed which is due to a damping of the SF (for a review see, e.g., Refs. 58 and 48). In a first approximation the electronic term γT is suppressed with increasing field. For our compounds, it has to be concluded that SFs either do not contribute much to the electronic specific heat or that the SFs are not measurably sensitive to fields.

The typical energy scale of the SF is given by Θ_p which varies between 80 K ($M=\text{Na}, \text{K}, \text{Tl}$) and 20 K ($M=\text{Ba}$).

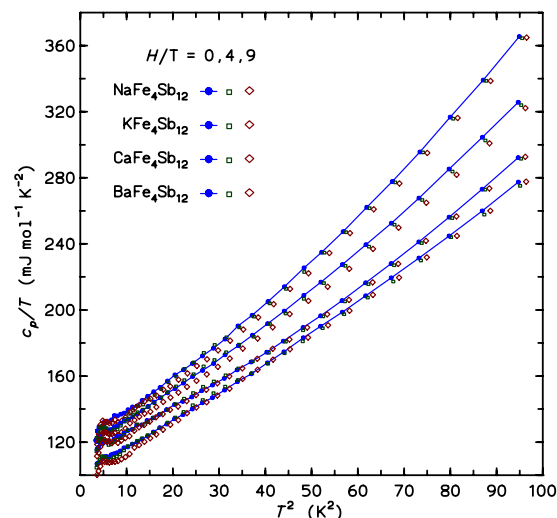


FIG. 7. (Color online) Magnetic field dependence of the specific heat ($c_p(T)/T$ vs T^2 representation) of filled skutterudites $M\text{Fe}_4\text{Sb}_{12}$ (from top to bottom: $M=\text{Na}, \text{K}, \text{Ca}, \text{Ba}$) below 10 K (see text).

Thus, especially for $\text{BaFe}_4\text{Sb}_{12}$ a significant SF contribution to γ might be expected. On the other hand, there is only a vague trend in γ (a decrease from ≈ 120 to ≈ 100 $\text{mJ mol}^{-1} \text{K}^{-1}$). Assuming similar values for γ (due to the similar DOS values at E_F),¹⁴ this would leave room only for a small contribution from SF (of order 10 $\text{mJ mol}^{-1} \text{K}^{-1}$) to γ of these compounds. Interestingly, only the ferromagnetic compounds with the slightly larger γ values actually display the small decrease of γ with increasing field. Thus, the effect is probably due to a damping of a ferromagnetic spin wave contribution ($c_{\text{SW}} \propto T^{3/2}$) in the ordered state.

In contrast, for the La compound samples ($y=0.79$ and 0.92), γ is almost twice that of the other compounds. In a $c_p(T)$ vs T^2 plot (Figs. 8 and 9) and also in the $\Delta c_p(T)$ plot in Fig. 5 a gradual upturn is visible below 50 K^2 indicating an

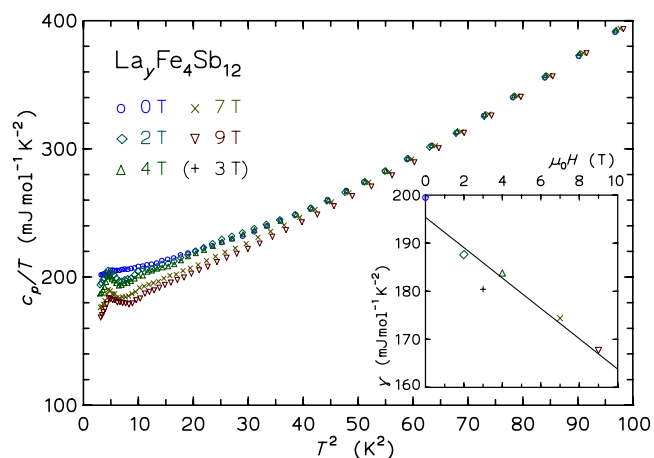


FIG. 8. (Color online) Magnetic field dependence of the specific heat ($c_p(T)/T$ vs T^2 representation) of $\text{La}_y\text{Fe}_4\text{Sb}_{12}$ ($y=0.79$) below 10 K. The inset shows $\gamma(H)$ (symbols) and a linear fit (line). The anomalies below $\approx 9 \text{ K}^2$ are due to an insufficiently calibrated field dependence of the temperature sensor.

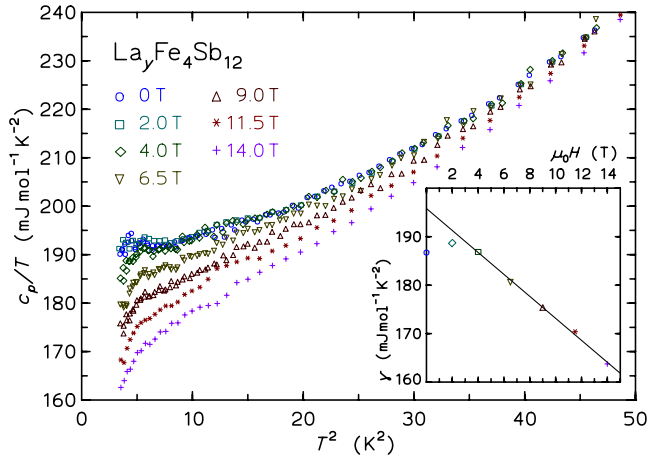


FIG. 9. (Color online) Magnetic field dependence of the heat capacity of $\text{La}_y\text{Fe}_4\text{Sb}_{12}$ ($y=0.92$) below 7 K.

additional contribution to $c_p(T)$. This contribution and the linear term decrease strongly with increasing field. The data for the $\text{La}_{0.79}\text{Fe}_4\text{Sb}_{12}$ crystal (Fig. 8) were fitted for fields of 0, 2, 3, 4, 6, and 9 T with two different models. A simple model $c_p(T, H) = \beta(H)T^3 + \delta(H)T^5 + \gamma(H)T$ could be applied to describe the data only in the limited temperature range of 3–7 K. The linear term γ of $195(3) \text{ mJ mol}^{-1} \text{ K}^{-2}$ at $H=0$ decreases with field approximately linearly by $-3.2(5) \text{ mJ mol}^{-1} \text{ K}^{-2} \text{ T}^{-1}$, i.e., $1.6(2) \times 10^{-2}/\text{T}$ (see inset of Fig. 8). Both values, $\gamma(0)$ and the slope, are in agreement with the findings of Viennois *et al.*³⁹

More successfully the data can be fitted with a model including additionally an Einstein term and a SF contribution $\sigma T^3 \ln(T/T_{\text{SF}})$ (Refs. 48 and 58) for the upturn of $\Delta c_p(T)$ (clearly visible in Fig. 5 below 8 K). A SF contribution of this temperature dependence has been observed, e.g., in Ni_3Al and UAl_2 .^{48,58} With the Einstein term the range of the fits could be extended to higher temperatures (here, 10 K). The reduced least-squares deviation of the fit for $H=0$ decreased to half the value when adding the SF term, underlining its significance. In order to obtain more reliable parameters (γ , β , and σ), the Einstein term for $\mu_0 H=9$ T was determined from the fit, and the optimal parameters $\epsilon = 17.2(1.1) \text{ J mol}^{-1} \text{ K}^{-1}$ and $\Theta_E = 76.4(1.6) \text{ K}$ were then fixed for all fits of data at lower fields. The resulting $\gamma(H)$ is—within error bars—identical to the one from fits with the simple model [$\gamma(H=0) = 198(2) \text{ mJ mol}^{-1} \text{ K}^{-2}$, slope $-3.6(4) \text{ mJ mol}^{-1} \text{ K}^{-2} \text{ T}^{-1}$].

In fits including both the βT^3 and a $\sigma T^3 \ln(T/T_{\text{SF}})$ contribution the coefficients β and σ are anticorrelated. Since we do not know the lattice Debye temperature and thus β_{lat} we have to extract it from the fit parameter β . Plotting the fitted β as function of σ results in a good linear relationship $\beta(\sigma) = \beta(0) - \sigma \ln T_{\text{SF}}$. From $\beta(0)$ a Debye temperature $\Theta_D = 264(2) \text{ K}$ is calculated while for the SF temperature $T_{\text{SF}} = 13(1) \text{ K}$ is found.

For the second single-crystal sample ($y=0.92$) measurements up to $\mu_0 H=14$ T were performed. The dependence of γ on H was slightly different. For this crystal, there is almost no decrease of γ for fields up to 4 T, a phenomenon

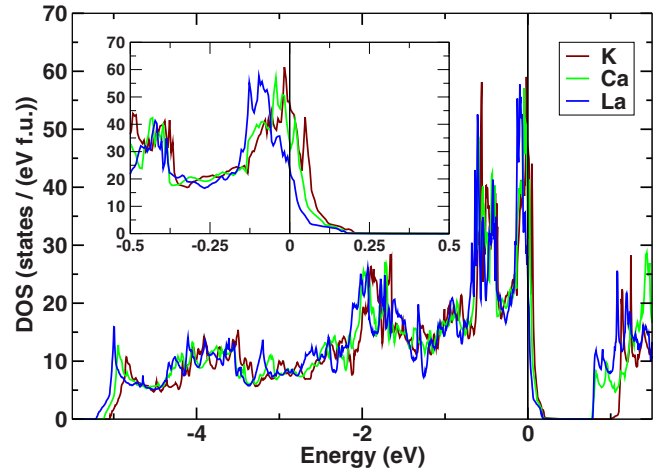


FIG. 10. (Color online) Comparison of the paramagnetic electronic DOS for $\text{KFe}_4\text{Sb}_{12}$, $\text{CaFe}_4\text{Sb}_{12}$, and $\text{LaFe}_4\text{Sb}_{12}$. The inset shows a magnification around E_F .

mentioned for several spin fluctuation compounds.^{48,58} Then a linear decrease of γ with a rate of $-2.3(1) \text{ mJ mol}^{-1} \text{ K}^{-2} \text{ T}^{-1}$, i.e., $1.2(1) \times 10^{-2}/\text{T}$ with $\gamma(H=0) = 196(1) \text{ mJ mol}^{-1} \text{ K}^{-2} \text{ T}^{-1}$ is observed. While $\gamma(H=0)$ is identical for both crystals the decrease of γ with H is weaker for the crystal with the larger occupancy of the La site. Again, the Einstein term for $\mu_0 H=14$ T was determined from the fit and these parameters $\epsilon = 15.1(7)$ and $\Theta_E = 68.7(6) \text{ K}$ were used for the fits at lower fields. β as function of σ again shows a good linear relation. A higher Debye temperature $\Theta_D = 298(1) \text{ K}$ is calculated and the energy scale for SF is also higher for the $\text{La}_{0.92}\text{Fe}_4\text{Sb}_{12}$ sample [$T_{\text{SF}} = 17(1) \text{ K}$] than for the $\text{La}_{0.79}\text{Fe}_4\text{Sb}_{12}$ sample, consistent with the smaller field dependence of γ for the La-rich sample.

The relatively low SF temperatures compared with the larger positive Weiss temperatures Θ_p of the skutterudites with mono- and divalent cations motivate the presence of the large SF contribution in the specific heat of $\text{La}_y\text{Fe}_4\text{Sb}_{12}$. The meaning of the sizable *negative* Θ_p from the susceptibility is, however, unclear in this respect. While from NMR measurements it was concluded that the SFs in $\text{La}_y\text{Fe}_4\text{Sb}_{12}$ are predominantly antiferromagnetic in character,⁴¹ a small energy reduction is still found for a ferromagnetic state in fixed spin moment calculations.¹⁴ From other NMR and NQR study Magishi *et al.*⁴² concluded that the SFs are ferromagnetic in $\text{La}_{0.88}\text{Fe}_4\text{Sb}_{12}$. Viennois *et al.*³⁹ also concluded from the low-temperature susceptibility that the SFs are of ferromagnetic character.

Since γ decreases linearly up to our maximum field it is impossible to derive an electronic γ from our experiments. The bare γ_0 derived from the DOS at E_F for $\text{LaFe}_4\text{Sb}_{12}$ is only $55 \text{ mJ mol}^{-1} \text{ K}^{-1}$ (see Fig. 10 and inset). Assuming a further increase of the enhancement of γ , as observed when going from the alkali to the alkaline-earth skutterudites, a value of $\gamma_0 \approx 100 \text{ mJ mol}^{-1} \text{ K}^{-2} \text{ T}^{-1}$ might be estimated,¹⁴ in agreement with the value of $110 \text{ mJ mol}^{-1} \text{ K}^{-2}$ derived in a similar way in Refs. 39 and 43.

The resulting value of Θ_D for the sample with the lower La occupancy is very similar to that of the skutterudites with

divalent fillers, e.g., $\text{BaFe}_4\text{Sb}_{12}$. This might be understood from the fact that the maximum charge transferred from the 0.79 La^{3+} ions to the polyanion is only $2.37e^-$, i.e., only little more than two electrons. Thus, the polyanion of $\text{La}_{0.79}\text{Fe}_4\text{Sb}_{12}$ is only a little “harder” than that of the skutterudites with Ca, Sr, Ba, or Yb. The significantly larger Θ_D for the $\text{La}_{0.92}\text{Fe}_4\text{Sb}_{12}$ crystal demonstrates that the chemical bond strength in the polyanion increases with increasing La occupancy and charge transfer.

For $M=\text{La}$ the Einstein temperature Θ_E is available—besides from ADPs (see Table I)—from several methods: *ab initio* phonon calculations by Feldman *et al.*⁵² give 7.1 meV (82 K) and inelastic neutron scattering measurements by Viennois *et al.*⁵⁹ and Feldman *et al.*⁵³ consistently yield ≈ 7 meV (81 K) for $\text{La}_{0.90-0.95}\text{Fe}_4\text{Sb}_{12}$,⁶⁰ all in fair agreement with our values (77 and 69 K, respectively, for two different La contents). Again, the coefficient ϵ of the Einstein term is less than $3Ry$ (for a discussion see Sec. III D).

F. Electrical resistivity and magnetoresistance

The electrical resistivity $\rho(T)$ of differently prepared compact samples of the seven skutterudites is given in the upper panel of Fig. 11. Here, the bulk density of the samples has a very strong influence on the absolute resistivity and the residual resistivity. Conventionally pressed and sintered samples with bulk densities well below theoretical density (as here the $\text{BaFe}_4\text{Sb}_{12}$ sample) have much higher room temperature and residual resistivities than our current SPS materials (at 0.6 GPa and 200–350 °C for 2 h). The SPS samples of $\text{KFe}_4\text{Sb}_{12}$ and $\text{NaFe}_4\text{Sb}_{12}$ have bulk densities of 92% and 93% of the density determined from the x-ray lattice parameters, respectively. They have resistivities well below that of previous less-dense material⁸ and near that of the two single-crystal samples. Subtracting the residual resistivity ρ_0 and normalizing at 300 K yield the curves in the lower panel of Fig. 11. The common feature of the normalized curves is the clear shoulder around 70–100 K. The shoulder is most pronounced for $M\text{Fe}_4\text{Sb}_{12}$ with divalent cations M and for $M=\text{Ba}$ it is at a higher temperature compared to $M=\text{Ca}, \text{Yb}$. The shoulder has vanished for $\text{La}_y\text{Fe}_4\text{Sb}_{12}$. In the ferromagnetic Na and K compounds the shoulder is overlaid by the small ordering anomaly at—most remarkably—the same temperature of $T_C \approx 80\text{K}$.

A shoulder in $\rho(T)$ at elevated temperature is often due to *s-d* scattering, where light charge carriers are scattered off more heavy electrons forming a narrow band near E_F . In order to check for the possible presence of different *s-d* scattering in the compounds, the partial DOS for *s* and *d* electrons at E_F were calculated.¹⁴ There is, however, no significant difference in the ratio of *s* and *d* DOS for the skutterudites with differently charged cations; thus, we have to abandon this explanation.

For the investigated compounds with divalent filler ions M an infrared pseudogap (with minimum at 12 meV for $M=\text{Ca}, \text{Sr}, \text{Yb}$ and 15 meV for $M=\text{Ba}$) was reported to appear at temperatures below ≈ 100 K. Such gap is not present in Na and K filled skutterudites^{19,61} and also does not exist for $\text{La}_y\text{Fe}_4\text{Sb}_{12}$ (see Fig. 10 inset). A closer inspection of the

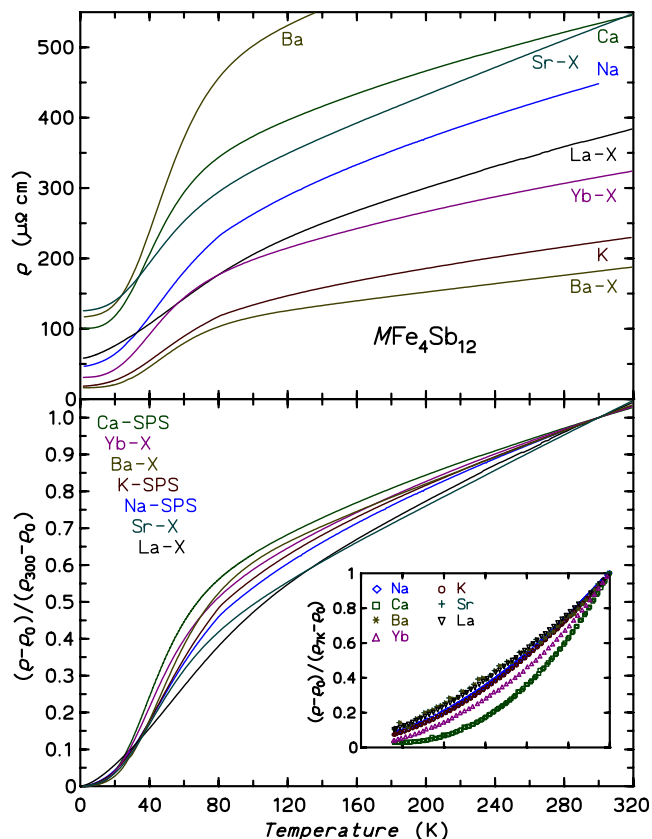


FIG. 11. (Color online) Electrical resistivity (upper) and normalized resistivity (lower panel) vs temperature of different filled skutterudites $M\text{Fe}_4\text{Sb}_{12}$ ($M=\text{Na}, \text{K}, \text{Sr}, \text{Ca}, \text{Ba}, \text{La}_{0.79}, \text{Yb}_{0.95}$). X assigns single crystal samples. The remaining samples were spark-plasma sintered (SPS). The inset shows normalized resistivity data ($\rho - \rho_0$) between 1 and 7 K.

spectral weight shift with temperature shows that the presence and the closing of the gap (by thermal smearing) lead to an increase of the dc resistivity below ≈ 100 K compared to compounds where no such pseudogap is present. The very pronounced shoulder of $\rho(T)$ of the skutterudites with divalent cations may thus be rationalized. Indeed, for $\text{BaFe}_4\text{Sb}_{12}$ the shoulder in $\rho(T)$ occurs at a higher temperature than for Ca, Yb, and Sr compounds, in agreement with the infrared spectroscopic data and detailed band structure calculations.¹⁹ The pseudogap can be explained by the fine details of the electronic structure which are well reproduced by calculations (see Fig. 10 inset). For more details we refer to Ref. 14.

The inset of Fig. 11 shows the low-temperature dependence of the normalized resistivity in zero field. It is evident that again a clear distinction can be made between the skutterudites with monovalent, divalent, and trivalent cations. $\rho(T, H)$ was fitted with power laws [plus $\rho_0(H)$] in temperature intervals with upper boundaries of 7 and 10 K. The resulting exponents $\alpha(H)$ are given in Table III. The surprisingly stable power law behavior is the $T^{1.9}$ dependence found for the ferromagnetically ordered Na and K compounds. α is even stable up to 20 K and increases from 1.9 in zero field to 2.0 in $\mu_0 H = 9$ T. This exponent is very close to the common T^2 dependence for a Fermi liquid.

TABLE III. Exponents α resulting from power-law fits of the resistivity $\rho(T)=\rho_0+AT^\alpha$ in magnetic fields H for the temperature interval 1.8–7 K. For $M=\text{Ba}$ the curve $\rho(T)$ shows a change of slope for fields of 2 and 4 T. The sample with $M=\text{Sr}$ show at the lowest temperatures an upturn of $\rho(T)$ in $\mu_0H=9$ T. Values of α determined from these data are given in parentheses.

| μ_0H (T) | Na | K | Ca | Sr | Ba | Yb | La |
|--------------|------|------|------|--------|--------|------|------|
| 0 | 1.88 | 1.93 | 3.11 | 2.49 | 1.97 | 2.30 | 1.68 |
| 2 | 1.92 | 1.89 | 2.45 | 2.52 | (1.52) | 2.04 | 1.68 |
| 4 | 1.93 | 1.92 | 2.28 | 2.52 | (1.32) | 1.98 | 1.72 |
| 9 | 2.04 | 1.96 | 2.31 | (2.75) | 2.26 | 1.91 | 1.80 |

In contrast, for the nearly ferromagnetic compounds with divalent cations (Ca, Yb), the T^2 dependence is only found for rather low temperatures. Fits with a higher upper limit of temperature display significantly larger exponents α . For $M=\text{Yb}$ there is a decrease of α from 2.59 to 2.30 when lowering the high-temperature limit. Most interestingly, for Ca a high exponent $\alpha \approx 3$ is essentially stable for intervals with high limits from 7 K up to 20 K. The low- T data for the Ba compound are of less good quality and start only at 3.9 K but show almost the same exponents as the Yb compound. $\rho(T, H)$ of all three compounds, however, displays a strong decrease of α with increasing magnetic field and recover the usual T^2 dependence in a wide temperature interval.

The observation of a temperature dependence stronger than T^2 in $\rho(T)$ for the skutterudites with divalent cations can be explained by an additional scattering mechanism which gets stronger with increasing temperature. This scattering manifests itself at elevated temperature as the pronounced shoulder in $\rho(T)$ and the unexpected exponents are thus a hallmark of the pseudogap at low temperatures. The gradual recovery of the T^2 behavior with increasing magnetic field can be understood by a closing or smearing of the pseudogap. Such a field behavior of the gap has actually been observed for the filled skutterudite $\text{CeRu}_4\text{Sb}_{12}$ by infrared reflectivity measurements.⁶²

The $\text{La}_y\text{Fe}_4\text{Sb}_{12}$ sample displays strongly different exponents α of 1.61–1.68 (in zero field) and no shoulder at higher temperatures. With increasing field α tends to slightly higher values but the T^2 law is clearly not achieved for the maximum field. The exponent is rather close to 5/3 which is typical for antiferromagnetic spin fluctuations.⁴⁰ This is in agreement with the negative sign of the Weiss parameter of the high-temperature susceptibility.

The ratio A/γ^2 [where A is the coefficient of the T^2 term in $\rho(T)=\rho_0+AT^2$] can only be calculated for Na and $\text{KFe}_4\text{Sb}_{12}$ in zero field and, eventually, for compounds with divalent M in high magnetic fields (where we observe such a law). The resulting values for $T < 7$ K are given in

Table IV. The values are between 0.13 and $0.37 \times 10^{-7} \Omega \text{ m} (\text{mol K/J})^2$; thus, they are significantly smaller than the free-electron Kadowaki-Woods value of $\approx 1 \times 10^{-7} \Omega \text{ m} (\text{mol K/J})^2$. Since just the lower resistivity and therefore the A values seem to be intrinsic it can be concluded that the ratio A/γ^2 of all $M\text{Fe}_4\text{Sb}_{12}$ is about $10^{-8} \Omega \text{ m} (\text{mol K/J})^2$.

Typical examples for the transverse magnetoresistance of a $M[\text{Fe}_4\text{Sb}_{12}]$ skutterudite are given in Fig. 12. For a plot of the quite similar behavior of the Ca and Yb compounds we refer to Fig. 4 of Ref. 15. The magnetoresistance (MR) is large and positive below ≈ 40 K and increases quadratically for low field and then changes over to a linear increase. For $\mu_0H=9$ T it reaches +37% in $\text{BaFe}_4\text{Sb}_{12}$ sinter and up to +73% for $\text{NaFe}_4\text{Sb}_{12}$. Similarly high values of MR were obtained for the other compounds, depending on the residual resistivity ρ_0 of the sample. This large MR is probably due to the low net charge carrier concentration (i.e., a strong compensation of hole- and electron-type charge carriers) in these filled skutterudites with mono- and divalent cations. In contrast, the MR of $\text{La}_y\text{Fe}_4\text{Sb}_{12}$ samples is low (maximal +1.4% at $T=2$ K and -0.7% at $T=30$ K in $\mu_0H=9$ T), confirming again that the La compound is electronically very different from the skutterudites with mono- and divalent cations.

G. Hall effect and band structure

Typical Hall resistivity ρ_H isotherms plotted against the field H are displayed for $\text{CaFe}_4\text{Sb}_{12}$ in Fig. 13. A correction for a residual component from transverse magnetoresistivity was taken into account. It can be seen that Hall resistivity behaves strongly nonlinear in field (below about 100 K), in spite of there being no magnetic order in $\text{CaFe}_4\text{Sb}_{12}$. Similar strong nonlinearity is observed in $\text{SrFe}_4\text{Sb}_{12}$ below ≈ 50 K, for $\text{Yb}_y\text{Fe}_4\text{Sb}_{12}$ below ≈ 80 K, and for the alkali-metal filled compounds in the whole temperature range. This is in contrast to isotherms measured on $\text{La}_y\text{Fe}_4\text{Sb}_{12}$ samples where ρ_H is indeed linear in field. Thus, the nonlinearity might be due

TABLE IV. Ratio A/γ^2 [in $10^{-8} \Omega \text{ m} (\text{mol K/J})^2$]. A was obtained from fits of the resistivity $\rho(T)$ with ρ_0+AT^2 in zero and 9 T magnetic field for the temperature interval 1.8–7 K.

| μ_0H (T) | Na | K | Ca | Sr | Ba | Yb | La |
|--------------|-------|-------|-------|----|-------|-------|----|
| 0 | 0.368 | 0.175 | | | 0.288 | | |
| 9 | 0.367 | 0.130 | 0.238 | | 0.294 | 0.088 | |

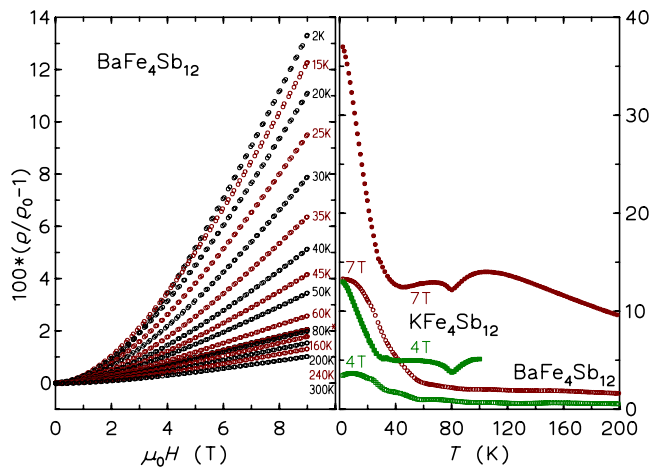


FIG. 12. (Color online) Left: transverse magnetoresistance $100 \times [\rho(H)/\rho(0) - 1]$ vs $\mu_0 H$ for a SPS sample of $\text{BaFe}_4\text{Sb}_{12}$. Isotherms at 80, 100, and 120 K are almost coinciding (marked by *). Right: temperature dependence of the magnetoresistance $100 \times (\rho/\rho_0 - 1)$ for the ferromagnetically ordering $\text{KFe}_4\text{Sb}_{12}$ (full symbols) and for paramagnetic $\text{BaFe}_4\text{Sb}_{12}$ (open symbols) for $\mu_0 H = 9$ and 4 T.

to the nearly ferromagnetic nature of the compounds. In order to get reliable values for the Hall coefficient only data at low fields (in the linear region) were used.

The low-field Hall coefficient $R_H(T)$ for the investigated skutterudite samples is given in Fig. 14. For the Na and K compounds strong anomalies around and below the ferromagnetic ordering temperature are visible which are due to skew scattering and which will not be discussed here further. A recent publication by Sales *et al.*⁶³ addresses in detail this anomalous Hall effect for the ferrimagnetic skutterudite compound $\text{Eu}_y\text{Fe}_4\text{Sb}_{12}$ (with ferromagnetic order of both the Eu and Fe sublattices).⁵⁵

All Hall resistivities R_H are positive; thus, holes are the majority charge carriers. Our band structure calculations¹⁴ indicate that the DOS at E_F is dominated by only two bands:

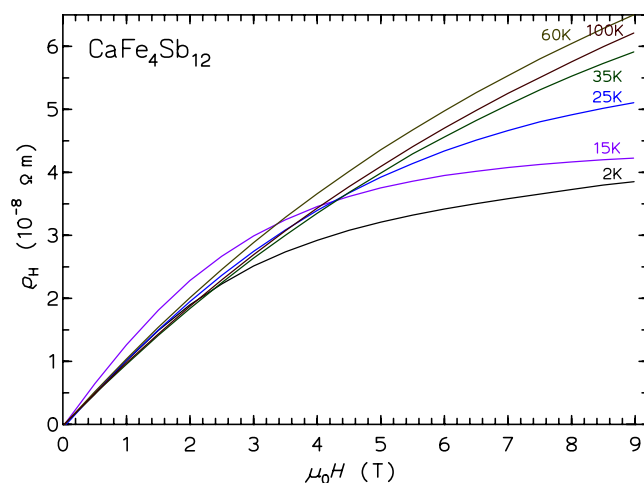


FIG. 13. (Color online) Selected isotherms ($T < 100$ K) of the Hall resistivity of polycrystalline $\text{CaFe}_4\text{Sb}_{12}$ vs field $\mu_0 H$.

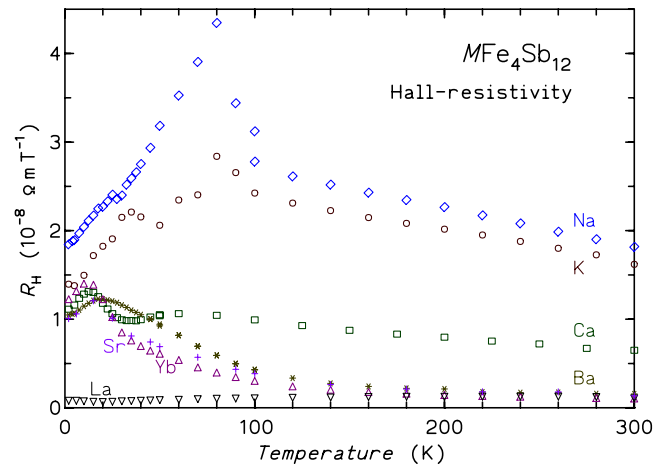


FIG. 14. (Color online) Hall coefficient of filled skutterudites $M\text{Fe}_4\text{Sb}_{12}$. The anomalies of the Na and K compound data in wide temperature range around 80 K are due the ferromagnetic ordering.

one with overall hole and the other with overall electron character. From the Hall data it is evident that the skutterudites with monovalent cations have the smallest effective charge carrier density and the compensation of hole and electron bands is nearly perfect ($N = 3.4$ and 3.9×10^{20} holes/cm³ at 300 K for Na and $\text{KFe}_4\text{Sb}_{12}$ within a one-band model, respectively). Similar values for R_H are found at the lowest temperatures, in spite of the anomalous Hall effect which is prominent for temperatures around T_C . The interpretation of the data is corroborated by the details of the band structure of $\text{KFe}_4\text{Sb}_{12}$. Figure 15 shows the Fermi surfaces of the bands relevant at the Fermi level. The contributions of these bands to the DOS are given in Fig. 16. In $\text{KFe}_4\text{Sb}_{12}$ the hole-type band (No. 174) and the electron-type band (No. 176) contribute the same DOS at E_F while band No. 175 has a mixed character. This leads to a strong compensation of charge carriers in this compound.

The compounds with divalent cations also show a similar Hall effect. $R_H(2 \text{ K})$ is between 1.0 and $1.3 \times 10^{-8} \Omega \text{ cm T}^{-1}$ corresponding to 5.6 (Ca), 5.9 (Ba, sinter), 7.3 (Ba-SPS), and $5.1 \times 10^{20}/\text{cm}^3$ (Yb, crystal) uncompensated holes. With increasing temperature—after going through a small maximum—the curves R_H for Ba and $\text{Yb}_y\text{Fe}_4\text{Sb}_{12}$ decrease strongly and at 300 K values corresponding to $N = 4.0$ (Ba-sinter), 2.0 (Ba-SPS), and 6.8 (Yb, crystal) $\times 10^{21}$ holes/cm³ are attained. $\text{La}_y\text{Fe}_4\text{Sb}_{12}$ shows only weakly temperature-dependent R_H with values corresponding to 6.8 and 5.2×10^{21} holes/cm³ at 2 and 300 K, respectively. The observations are compatible with the details of the band structure at E_F (see Figs. 15 and 16). For $\text{CaFe}_4\text{Sb}_{12}$ there are more holes from band No. 175 than electrons from band No. 176. A significant compensation of holes by electrons is therefore found for $\text{CaFe}_4\text{Sb}_{12}$ (and the other skutterudites with divalent M). Finally, for $\text{La}_y\text{Fe}_4\text{Sb}_{12}$, with even more electrons transferred to the $[\text{Fe}_4\text{Sb}_{12}]$ polyanion, the hole-type band No. 176 almost exclusively forms the Fermi surface. No charge carrier compensation is thus present and the Hall coefficient is relatively low for $\text{La}_y\text{Fe}_4\text{Sb}_{12}$ in comparison to the compounds with divalent cations.

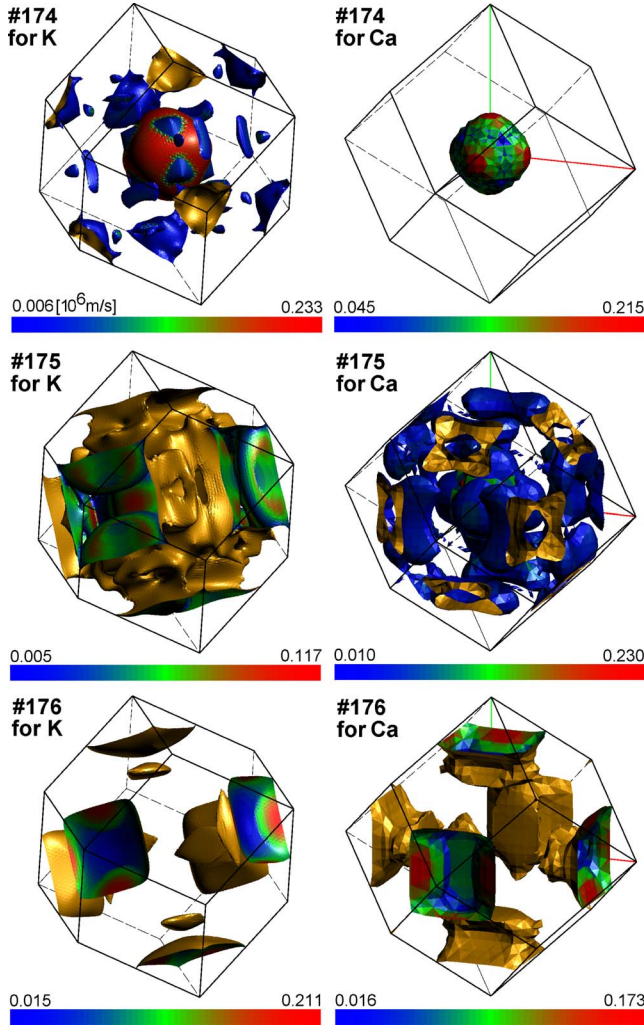


FIG. 15. (Color online) Fermi surfaces for band Nos. 174, 175, and 176 of $\text{KFe}_4\text{Sb}_{12}$ (left) and of $\text{CaFe}_4\text{Sb}_{12}$ (right). Color encodes the Fermi velocity (in 10^{-6} m/s) for the electron-type carriers; golden color indicates the outside of (electron-filled) Fermi surfaces. Thus, outer surfaces with the golden color indicate an electronlike character of the band for these k vectors.

Interestingly, $\text{CaFe}_4\text{Sb}_{12}$ displays a weaker decrease of R_H with increasing temperature ($N=9.6 \times 10^{20}$ holes/ cm^3) and a local minimum of R_H around 35 K. This temperature is similar to that of the hump observed in $\chi(T)$ (see Figs. 2 and 1 in Ref. 15) of the nearly ferromagnetic skutterudites and is also probably due to spin fluctuations.

IV. CONCLUSIONS

The seven differently charged nonmagnetic cations ($M = \text{Na}, \text{K}, \text{Ca}, \text{Sr}, \text{Ba}, \text{La}, \text{Yb}$) used in this study on $M_y\text{Fe}_4\text{Sb}_{12}$ feature a wide range of atomic mass and size. All these cations (and also thallium) are compatible with the icosahedral cage in the $[\text{Fe}_4\text{Sb}_{12}]$ polyanion. With increasing charge of the cation more charge is transferred to the polyanion, changing its electronic ground state. While we did not succeed in preparing samples with an incomplete occupation of the cat-

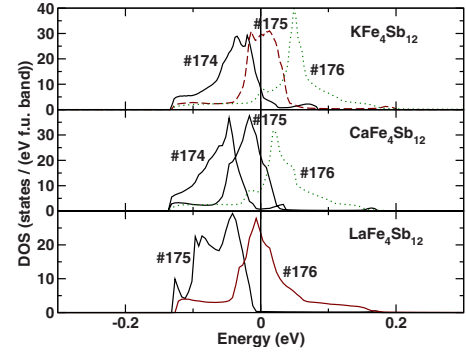


FIG. 16. (Color online) Band resolved density of states (DOS) for $\text{KFe}_4\text{Sb}_{12}$, $\text{CaFe}_4\text{Sb}_{12}$, and $\text{LaFe}_4\text{Sb}_{12}$ for energies around the Fermi level. The numbering of the bands corresponds to the Fermi surfaces shown in Fig. 15. Their character is indicated by the line styles: full—holelike, dotted—electronlike, and dot dashed—mixed character.

ion site by monovalent ions the compounds with trivalent ions are prone to have defects on this position. The maximum charge transfer from the cation to the $[\text{Fe}_4\text{Sb}_{12}]$ unit seems to be close to three.

Electronic properties vary systematically with the charge transferred to the host. While the host with one additional electron is generally (weakly itinerant) ferromagnetic with a $T_C \approx 80$ K, the compounds with divalent cations are nearly ferromagnetic with strong spin fluctuations. It is possible to quench these spin fluctuations and to drive these materials toward ordering. One way is the itinerant electron metamagnetic transition, i.e., application of high magnetic fields,⁴⁴ another is the incorporation of (divalent) ions with strong local magnetic moments such as europium (Eu^{2+} with $S = 7/2$).⁵⁵ In the latter case a ferrimagnetic arrangement of the Eu and Fe spins is achieved with $T_C \approx 86$ K, i.e., at a temperature slightly higher than in the compounds with monovalent cations. The induced fields $\mu_0 H_{\text{ind}}$ as observed by Mössbauer spectroscopy in $\text{NaFe}_4\text{Sb}_{12}$ ($\mu_0 H_{\text{ind}} = 1.64$ T)⁹ and in $\text{TlFe}_4\text{Sb}_{12}$ ($\mu_0 H_{\text{ind}} = 0.7$ T [majority component] and 1.8 T [minority component])¹⁰ are small. For $\text{Eu}_{0.88}\text{Fe}_4\text{Sb}_{12}$ similarly small $\mu_0 H_{\text{ind}}$ values with opposite sign were observed,⁶⁴ indicating that the Fe magnetism in the Eu compound and in $M^{1+}\text{Fe}_4\text{Sb}_{12}$ ($M^{1+} = \text{Na}, \text{K}, \text{Tl}$) is based on the same physics.

Finally, for more than two transferred electrons, the tendency toward ferromagnetic ordering almost completely ceases (in case of $\text{LaFe}_4\text{Sb}_{12}$ fixed-spin moment calculations still indicate a tiny energy gain for a ferromagnetic moment of $\approx 0.24\mu_B$).¹⁴ While the density of states at E_F decreases in the sequence of the ions $\text{K}^{1+}-\text{Ca}^{2+}-\text{La}^{3+}$ the enhancement (from a comparison with the electronic specific heat coefficient γ) increases. While strong electronic correlations play no role in $\text{Na}/\text{K}/\text{TlFe}_4\text{Sb}_{12}$ the La compound is a metal with enhanced electronic correlations and γ raised by about a factor of 2 over the value derived from the calculated DOS. This large electronic specific heat coefficient is significantly lowered by magnetic fields, highlighting the large influence of spin fluctuations in $\text{La}_y\text{Fe}_4\text{Sb}_{12}$. For high fields γ is suppressed linearly with field and spin fluctuation temperatures T_{SF} of 13(1) and 17(1) K are obtained, depending on the

filling level y . The character of the spin fluctuations is, however, not yet fully clarified.

Equally as the electronic ground state the phononic properties could be systematically evaluated for compounds with (isoelectronic) cations of strongly different masses. The stiffness of the host structure increases with the number of transferred electrons as demonstrated by the increasing Debye temperatures. The physics of the vibrations of the cation in its large cavity is more complicated and cannot be captured by a simple (localized) Einstein oscillator picture. From the spectral weight contained in the Einstein mode observed in specific heat data of the compounds with heavier cations ($M = \text{Yb, Tl}$) it can be concluded that higher-energy contributions exist which indicate a significant hybridization with antimony modes of the cage. This hybridization of the vibrations of the cation and of the host is expected to be much stronger in skutterudites with cations of mass comparable or lighter than antimony.

The electronic transport properties of the compounds of this series also mirror their (calculated) electronic structure. The large Hall coefficients of the skutterudites with mono- and divalent cations are due to strong compensation of hole and electron carriers from up to three bands. This is a consequence of the different characters of these bands as could be shown by detailed Fermi surface calculations. The calculated Fermi surface sheets of $\text{KFe}_4\text{Sb}_{12}$ and $\text{CaFe}_4\text{Sb}_{12}$ show very different characters with respect to the relevant charge carriers (holes versus electrons) and strong anisotropies in the corresponding Fermi velocity. This explains at least

qualitatively the observed large Hall coefficients due to the resulting strong compensation. In contrast, for $\text{LaFe}_4\text{Sb}_{12}$ a single Fermi surface sheet with hole character is dominating the transport properties, resulting in a much smaller Hall coefficient.

The hump in the temperature dependence of the resistivity of $M\text{Fe}_4\text{Sb}_{12}$ ($M = \text{Ca, Sr, Ba, Yb}$) at ≈ 80 K and the nonquadratic variation of $\rho(T)$ at low temperatures are connected to a pseudogap which vanishes at ≈ 100 K. This pseudogap has been observed in the optical conductivity and is due to a common characteristic feature in the band structure of these compounds.¹⁹ The attribution of the pseudogap on a band structure effect proves that compounds such as $\text{Yb}_3\text{Fe}_4\text{Sb}_{12}$ are not at all governed by strong electronic correlations.

The electronic and phononic properties of the new compound $\text{TlFe}_4\text{Sb}_{12}$ with monovalent Tl^{1+} ions¹⁰ perfectly fit into this systematics. We also expect that this picture of the electronic state of the $[\text{Fe}_4\text{Sb}_{12}]$ polyanion holds when incorporating magnetic ions, e.g., rare-earth ions. In this case the subtle magnetic properties of the d -electron system will be modified and obscured by the rare-earth magnetism.

ACKNOWLEDGMENTS

We are indebted to N. Reinfried, U. Burkhardt, M. Baenitz, and R. Koban (all at MPI-CPfS). We thank M. M. Koza (ILL Grenoble) for fruitful discussions. H.R. acknowledges the Deutsche Forschungsgemeinschaft (Emmy-Noether-Programm) for financial support.

*jasper@cpfs.mpg.de

[†]Permanent address: II. Physikalisches Institut, Universität zu Köln, Zùlpicher Straße 77, 50937 Köln, Germany.

¹W. Jeitschko and D. Braun, *Acta Crystallogr., Sect. B: Struct. Crystallogr. Cryst. Chem.* **33**, 3401 (1977).

²C. Uher, *Semicond. Semimetals* **68**, 139 (2001).

³I. Shirovani, Y. Shimaya, K. Kihou, C. Sekine, N. Takeda, M. Ishikawa, and T. Yagi, *J. Phys.: Condens. Matter* **15**, S2201 (2003).

⁴E. D. Bauer, N. A. Frederick, P.-C. Ho, V. S. Zapf, and M. B. Maple, *Phys. Rev. B* **65**, 100506(R) (2002).

⁵N. A. Frederick, T. D. Do, P.-C. Ho, N. P. Butch, V. S. Zapf, and M. B. Maple, *Phys. Rev. B* **69**, 024523 (2004).

⁶G. A. Slack and V. G. Tsoukala, *J. Appl. Phys.* **76**, 1665 (1994).

⁷B. C. Sales, in *Handbook on the Physics and Chemistry of Rare Earths*, edited by K. A. Gschneidner, Jr., J.-C. G. Bünzli, and V. K. Pecharsky (Elsevier, Amsterdam, 2003), Vol. 33, Chap. 211, pp. 1–34.

⁸A. Leithe-Jasper, W. Schnelle, H. Rosner, N. Senthilkumaran, A. Rabis, M. Baenitz, A. Gippius, E. Morozova, J. A. Mydosh, and Yu. Grin, *Phys. Rev. Lett.* **91**, 037208 (2003); **93**, 089904(E) (2004).

⁹A. Leithe-Jasper, W. Schnelle, H. Rosner, M. Baenitz, A. Rabis, A. A. Gippius, E. N. Morozova, H. Borrmann, U. Burkhardt, R. Ramlau, U. Schwarz, J. A. Mydosh, Yu. Grin, V. Ksenofontov, and S. Reiman, *Phys. Rev. B* **70**, 214418 (2004).

¹⁰A. Leithe-Jasper, W. Schnelle, H. Rosner, R. Cardoso-Gil, M. Baenitz, J. A. Mydosh, Yu. Grin, M. Reissner, and W. Steiner, *Phys. Rev. B* **77**, 064412 (2008).

¹¹J. M. D. Coey and S. Sanvito, *J. Phys. D* **37**, 988 (2004).

¹²G. Sheet, H. Rosner, S. Wirth, A. Leithe-Jasper, W. Schnelle, U. Burkhardt, J. A. Mydosh, P. Raychaudhuri, and Yu. Grin, *Phys. Rev. B* **72**, 180407(R) (2005).

¹³M. E. Danebrock, C. B. Evers, and W. Jeitschko, *J. Phys. Chem. Solids* **57**, 381 (1996).

¹⁴H. Rosner, A. Leithe-Jasper, W. Schnelle *et al.* (unpublished).

¹⁵W. Schnelle, A. Leithe-Jasper, M. Schmidt, H. Rosner, H. Borrmann, U. Burkhardt, J. A. Mydosh, and Yu. Grin, *Phys. Rev. B* **72**, 020402(R) (2005).

¹⁶E. Matsuoka, K. Hayashi, A. Ikeda, K. Tanaka, T. Takabatake, and M. Matsumura, *J. Phys. Soc. Jpn.* **74**, 1382 (2005).

¹⁷M. Matsumura, G. Hyoudou, H. Kato, R. Nishioka, E. Matsuoka, H. Tou, T. Takabatake, and M. Sera, *J. Phys. Soc. Jpn.* **74**, 2205 (2005).

¹⁸T. Takabatake, E. Matsuoka, S. Narazu, K. Hayashi, S. Morimoto, T. Sakakawa, K. Umeo, and M. Sera, *Physica B* **383**, 93 (2006).

¹⁹J. Sichelschmidt, V. Voevodin, H. J. Im, S. Kimura, H. Rosner, A. Leithe-Jasper, W. Schnelle, U. Burkhardt, J. A. Mydosh, Yu. Grin, and F. Steglich, *Phys. Rev. Lett.* **96**, 037406 (2006).

²⁰H. Bonrath, K. H. Hellwege, K. Nicolay, and G. Weber, *Phys. Kondens. Mater.* **4**, 382 (1966).

²¹T. Ikeno, A. Mitsuda, T. Miuzshima, T. Kuwal, Y. Isikawa, and I.

- Tamura, J. Phys. Soc. Jpn. **76**, 024708 (2007).
- ²²Y. S. Dedkov, S. L. Molodtsov, H. Rosner, A. Leithe-Jasper, W. Schnelle, M. Schmidt, and Yu. Grin, Physica C **460-462**, 698 (2007).
- ²³G. K. White and M. L. Mingos, Int. J. Thermophys. **18**, 1269 (1997).
- ²⁴J. Ihringer and A. Küster, J. Appl. Crystallogr. **26**, 135 (1993).
- ²⁵L. G. Akselrud, P. Y. Zavalii, Yu. Grin, V. K. Pecharsky, B. Baumgartner, and E. Wölfel, Mater. Sci. Forum **133-136**, 335 (1993).
- ²⁶G. M. Sheldrik, SHELXL-97, University of Göttingen, Göttingen, 1997.
- ²⁷K. Koepf and H. Eschrig, Phys. Rev. B **59**, 1743 (1999).
- ²⁸J. P. Perdew and Y. Wang, Phys. Rev. B **45**, 13244 (1992).
- ²⁹H. Eschrig, *Optimized LCAO Method and the Electronic Structure of Extended Systems* (Springer, Berlin, 1989).
- ³⁰J. W. Kaiser and W. Jeitschko, J. Alloys Compd. **291**, 66 (1999).
- ³¹N. T. Stetson, S. M. Kauzlarich, and H. Hope, J. Solid State Chem. **91**, 140 (1991).
- ³²B. C. Sales, B. C. Chakoumakos, D. Mandrus, J. W. Sharp, N. R. Dilley, and M. B. Maple, in *Thermoelectric Materials 1998—The Next Generation Materials for Small Scale Refrigeration and Power Generation Applications*, edited by T. M. Tritt, M. G. Kanatzidis, G. D. Mahan, and H. B. Lyon, Jr. (Materials Research Society, Warrendale, PA, 1998), Vol. 545, p. 13.
- ³³G. S. Nolas, G. A. Slack, D. T. Morelli, T. M. Tritt, and A. C. Ehrlich, J. Appl. Phys. **79**, 4002 (1996).
- ³⁴R. D. Shannon, Acta Crystallogr., Sect. A: Cryst. Phys., Diffr., Theor. Gen. Crystallogr. **32**, 751 (1976).
- ³⁵P. Ghosez and M. Veithen, J. Phys.: Condens. Matter **19**, 096002 (2007).
- ³⁶B. C. Sales, D. Mandrus, and B. C. Chakoumakos, Semicond. Semimetals **70**, 1 (2001).
- ³⁷B. C. Sales, B. C. Chakoumakos, D. Mandrus, and J. W. Sharp, J. Solid State Chem. **146**, 528 (1999).
- ³⁸P. W. Selwood, *Magnetochemistry*, 2nd ed. (Interscience, New York, 1956).
- ³⁹R. Viennois, S. Charar, D. Ravot, P. Haen, A. Mauger, A. Bontien, S. Paschen, and F. Steglich, Eur. Phys. J. B **46**, 257 (2005).
- ⁴⁰T. Moriya, *Spin Fluctuations in Itinerant Electron Magnetism* (Springer-Verlag, Berlin, 1985).
- ⁴¹A. Gippius, M. Baenitz, E. Morozova, A. Leithe-Jasper, W. Schnelle, A. Shevelkov, E. Alkaev, A. Rabis, J. Mydosh, Yu. Grin, and F. Steglich, J. Magn. Magn. Mater. **300**, 403(E) (2006).
- ⁴²K. Magishi, Y. Nakai, K. Ishida, H. Sugawara, I. Mori, T. Saito, and K. Koyama, J. Phys. Soc. Jpn. **75**, 023701 (2006).
- ⁴³K. Nouneh, A. H. Reshak, S. Auluck, I. V. Kityk, R. Viennois, S. Benet, and S. Charar, J. Alloys Compd. **437**, 39 (2007).
- ⁴⁴S. Yoshii, E. Matsuoka, K. Hayashi, T. Takabatake, M. Hagiwara, and K. Kindo, Physica B **378-380**, 241 (2006).
- ⁴⁵V. Keppens, D. Mandrus, B. C. Sales, B. C. Chakoumakos, P. Day, R. Coldea, M. B. Maple, D. A. Gajewski, E. J. Freeman, and S. Benington, Nature (London) **395**, 876 (1998).
- ⁴⁶R. P. Hermann, R. Jin, W. Schweika, F. Grandjean, D. Mandrus, B. C. Sales, and G. J. Long, Phys. Rev. Lett. **90**, 135505 (2003).
- ⁴⁷E. S. R. Gopal, *Specific Heat at Low Temperatures* (Plenum, London, 1966).
- ⁴⁸A. Tari, *The Specific Heat of Matter at Low Temperatures* (Imperial College Press, London, 2003).
- ⁴⁹T. H. K. Barron and G. K. White, *Heat Capacity and Thermal Expansion at Low Temperatures* (Kluwer, Dordrecht/Plenum, New York, 1999).
- ⁵⁰D. Cao, F. Bridges, P. Chesler, S. Bushart, E. D. Bauer, and M. B. Maple, Phys. Rev. B **70**, 094109 (2004).
- ⁵¹G. J. Long, R. P. Hermann, F. Grandjean, E. E. Alp, W. Sturhahn, C. E. Johnson, D. E. Brown, O. Leupold, and R. Ruffer, Phys. Rev. B **71**, 140302(R) (2005).
- ⁵²J. L. Feldman, D. J. Singh, C. Kendziora, D. Mandrus, and B. C. Sales, Phys. Rev. B **68**, 094301 (2003).
- ⁵³J. L. Feldman, P. Dai, T. Enck, B. C. Sales, D. Mandrus, and D. J. Singh, Phys. Rev. B **73**, 014306 (2006).
- ⁵⁴W. Schnelle (unpublished).
- ⁵⁵V. V. Krishnamurthy, J. C. Lang, D. Haskel, D. J. Keavney, G. Srajer, J. L. Robertson, B. C. Sales, D. G. Mandrus, D. J. Singh, and D. I. Bilc, Phys. Rev. Lett. **98**, 126403 (2007).
- ⁵⁶M. M. Koza (private communication).
- ⁵⁷H.-C. Wille, R. P. Hermann, I. Sergueev, O. Leupold, P. van der Linden, B. C. Sales, F. Grandjean, G. J. Long, R. Ruffer, and Y. V. Shvyd'ko, Phys. Rev. B **76**, 140301(R) (2007).
- ⁵⁸K. Ikeda, S. K. Dhar, M. Yoshizawa, and K. A. Gschneidner, Jr., J. Magn. Magn. Mater. **100**, 292 (1991).
- ⁵⁹R. Viennois, L. Girard, D. Ravot, H. Mutka, M. Koza, F. Terki, S. Charar, and J. C. Tedenac, Physica B **350**, 403(E) (2004).
- ⁶⁰R. Viennois (private communication).
- ⁶¹S. Kimura, T. Mizuno, H. Im, K. Hayashi, E. Matsuoka, and T. Takabatake, Phys. Rev. B **73**, 214416 (2006).
- ⁶²S. V. Dordevic, K. S. D. Beach, N. Takeda, Y. J. Wang, M. B. Maple, and D. N. Basov, Phys. Rev. Lett. **96**, 017403 (2006).
- ⁶³B. C. Sales, R. Jin, D. Mandrus, and P. Khalifah, Phys. Rev. B **73**, 224435 (2006).
- ⁶⁴M. Reissner, E. Bauer, W. Steiner, G. Hilscher, A. Grytsiv, and P. Rogl, Physica B **378-380**, 232 (2006).